

# Ground Engineering using Prefabricated Vertical Drains: A Review

V.A. Sakleshpur, M. Prezzi, and R. Salgado  
*Lyles School of Civil Engineering, Purdue University, West Lafayette, IN, USA*  
*E-mail: vsaklesh@purdue.edu*

**ABSTRACT:** Improvement of soft ground by preloading with prefabricated vertical drains (PVDs) is a common practice in the field of ground engineering. PVDs accelerate the consolidation process of soft soils by providing a shorter drainage path for the pore water and thereby increase the strength and stiffness of soft soils over time. This paper presents a review of recent analytical, laboratory, numerical and field studies performed using preloading with PVDs for improvement of soft ground. The focus of the paper is on conventional PVDs without the use of vacuum, thermal and electro-osmosis techniques. Summary tables, which provide quick and easy access to the latest information from various research efforts, have been prepared and discussed. The review is complemented by two case histories that highlight the performance of PVDs in the field.

**KEYWORDS:** Ground improvement, Prefabricated vertical drain (PVD), Inner smear zone, Transition zone, Well resistance, Case history

## 1. INTRODUCTION

Soft soils, such as soft estuarine and marine clays, peats, and marshy soils, encountered commonly along deltaic and coastal regions throughout the world, are highly compressible in nature and possess undesirable geotechnical properties, such as high natural moisture content (close to the liquid limit), low undrained shear strength and low hydraulic conductivity. Therefore, structures constructed on these soils face problems of stability and serviceability if measures are not taken to improve them. Although pile foundations may be adopted in some situations to overcome these problems, they may be too expensive, especially for supporting embankments and low-to-medium-rise buildings. In such cases, the soil within the load transfer zone of the structure needs to be improved to make the ground suitable to support the applied load. Ground improvement essentially means increasing the shear strength and reducing the compressibility of the soil to the desired extent. Several soft ground engineering techniques, such as preloading alone, preloading with vertical drains, vacuum consolidation, stone columns, and deep soil mixing, have been used throughout the world.

Among all these techniques, preloading is the simplest and most economical method of inducing settlement so that a structure constructed on improved ground does not settle excessively. Preloading is achieved by placing a temporary surcharge, such as earth fill or sand bags, over soft ground prior to the construction of the proposed structure (Figure 1). The magnitude of the surcharge is typically higher than the preconsolidation pressure of soft soil so that it is forced to consolidate along the normal consolidation line. The soil gradually gains strength and stiffness over time. However, a major limitation of preloading is the time needed to achieve the required degree of consolidation, which is often so large (typically decades) that no construction project has the luxury of waiting that long. Provision of vertical drains, as shown in Figure 2, reduces the time required for consolidation of soft soil, and thus the two techniques combined, preloading with vertical drains, is one of the most preferred methods for improvement of soft ground.

Preloading with vertical drains accelerates the primary consolidation of soft soil due to two mechanisms. Firstly, the drains are often spaced closely (equal to 1 to 2 m in the case of strip or prefabricated vertical drains (PVDs)), and thus the maximum length of the pore water drainage path reduces to about half of the PVD spacing, which is usually a small fraction of the thickness of the soil layer. Secondly, the direction of flow of pore water changes from vertical (for preloading alone; Figure 1) to horizontal (for preloading with vertical drains; Figure 2). Most sedimentary deposits exhibit anisotropy with respect to the hydraulic conductivity in such a way that the horizontal component is at least twice that of the vertical component. Therefore, the coefficient of consolidation for flow of pore water in the horizontal direction is higher than that

corresponding to flow in the vertical direction. Because of these two effects, the time needed to achieve the required degree of consolidation reduces to a few months instead of decades in the case of preloading alone (Figure 3).

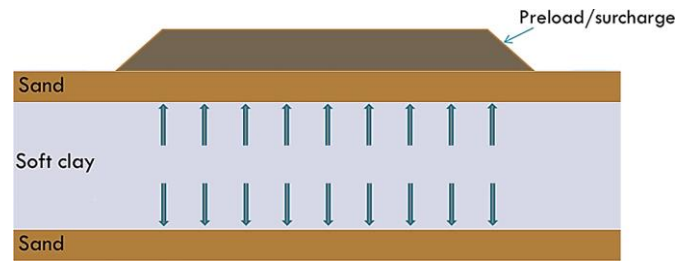


Figure 1 Preloading

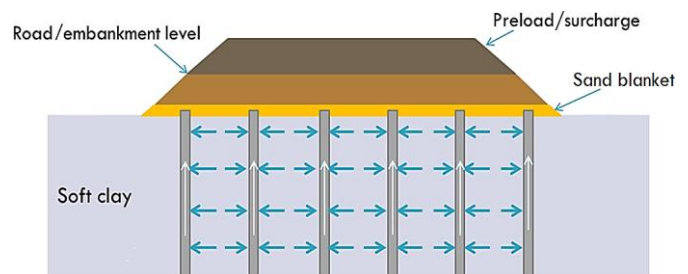


Figure 2 Preloading with vertical drains

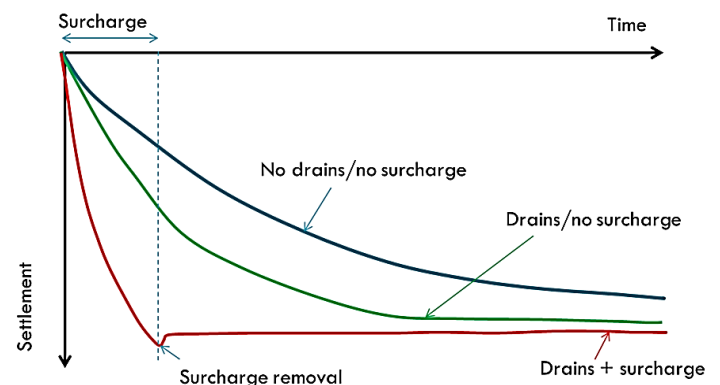


Figure 3 Typical time-settlement curves for different combinations of ground improvement

The earliest form of vertical drains was sand drains, which consisted of a borehole filled with sand. Dastidar *et al.* (1969) introduced sand-wicks, which were beneficial over sand drains with respect to: (a) ease of construction, (b) reduced smear effect, due to smaller drain cross-section, and (c) drain continuity. Since the 1970s, band-shaped PVDs, originally developed by Kjellman (1948), have replaced sand-wicks. A typical PVD has a width of 100 mm and a thickness of 3 to 4 mm. It consists of a thin geotextile filter sleeve, typically non-woven, surrounding a corrugated or studded plastic central core. The filter sleeve prevents fine soil particles from entering the core, but allows easy infiltration of pore water. The central core acts as a drainage channel while withstanding buckling and compressive stresses. Thus, the primary functions of PVDs are: (a) to filter the excess pore water from the consolidating soil (filtration), and (b) to carry the pore water away from the soil layers by vertical flow (drainage) through the drain (Basu and Madhav 2000).

**1.1 Equivalent Radius of Unit Cell**

PVDs are typically installed in square or triangular patterns (Figure 4) using a mandrel (Figure 5), which is square, rectangular, or octagonal in shape. For PVDs installed in rectangular, square or triangular patterns, the corresponding unit cells are rectangular, square or hexagonal in shape (in plan). For a rectangular installation pattern, the equivalent radius  $r_{c,eq}$  of the unit cell is given by

$$r_{c,eq} = \sqrt{\frac{s_x s_y}{\pi}} \tag{1}$$

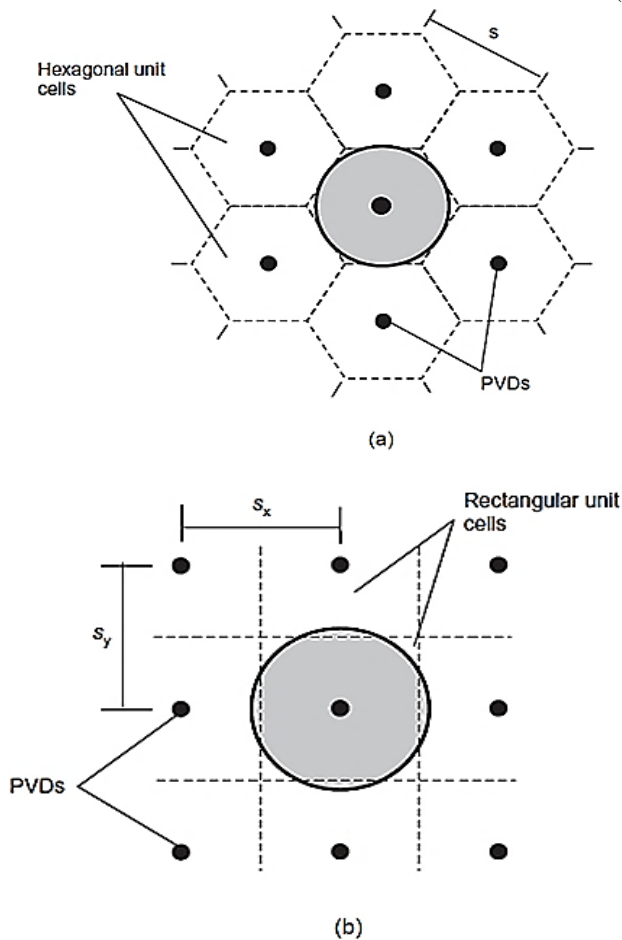


Figure 4 Installation patterns of PVDs: (a) triangular and (b) square (when  $s_x = s_y$ ) (Basu *et al.* 2010a)

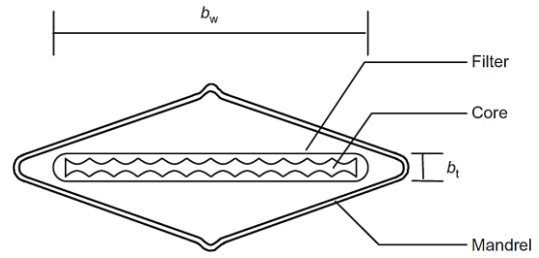


Figure 5 PVD enclosed by mandrel (Basu *et al.* 2010a)

where  $s_x$  and  $s_y$  are the centre-to-centre spacings of the PVDs in two mutually perpendicular directions. Equation (1) can also be used to calculate  $r_{c,eq}$  for a square installation pattern by making  $s_x = s_y$ . For a triangular installation pattern with centre-to-centre spacing  $s$ , the equivalent radius of the unit cell is given by

$$r_{c,eq} = \sqrt{\frac{\sqrt{3}}{2\pi}} s \tag{2}$$

**1.2 Equivalent Radius of PVD**

Hansbo (1979) proposed that the equivalent radius  $r_{d,eq}$  of a PVD of width  $b_w$  and thickness  $b_t$  can be determined by equating the perimeter of the actual band shape with that of an equivalent circle as

$$r_{d,eq} = \frac{b_w + b_t}{\pi} \tag{3}$$

Subsequent research has shown that, due to the corner effect, the equivalent radius of a PVD would be less than the value calculated based on an equal perimeter assumption (Eq. (3)). Based on finite element analyses, Rixner *et al.* (1986) proposed an alternate expression for the equivalent radius of a PVD as

$$r_{d,eq} = \frac{b_w + b_t}{4} \tag{4}$$

Rixner *et al.* (1986) recommend the use of Eq. (4) for values of the ratio  $b_w/b_t$  equal to 50 or less. Equations (3) and (4) are commonly used in practice, among several others reported in the literature (Abuel-Naga and Bouazza 2009), for estimation of the equivalent radius of a PVD.

**1.3 PVD-Induced Soil Disturbance**

In the field, the PVD is placed inside a mandrel and then pushed into the ground at a certain installation rate with the help of a rig. Once the desired depth is reached, the mandrel is withdrawn, leaving the PVD in the ground. During the insertion and withdrawal of the mandrel, a zone of soil around the PVD gets disturbed and sometimes completely remoulded. Consequently, the horizontal hydraulic conductivity of soil in this disturbed zone is less than the *in situ* or undisturbed horizontal hydraulic conductivity  $k_h$ . This reduction in horizontal hydraulic conductivity due to soil disturbance causes a decrease in the consolidation rate. In this paper, the disturbed zone is considered to consist of two distinct zones (Figure 6), namely, the inner smear zone and the transition zone (sometimes referred to as the outer smear zone), following Basu *et al.* (2010a).

The equivalent radii of the inner smear zone and the transition zone, measured from the center of the PVD, are denoted by  $r_{sm}$  and  $r_{tr}$ , respectively, and the horizontal hydraulic conductivities of soil

in the inner smear zone and the transition zone are denoted by  $k_{sm}$  and  $k_{tr}$ , respectively. The separation of the disturbed zone into the inner smear zone and the transition zone is not always done in routine analyses; a single disturbed zone is commonly referred to in the literature as the “smear zone”.

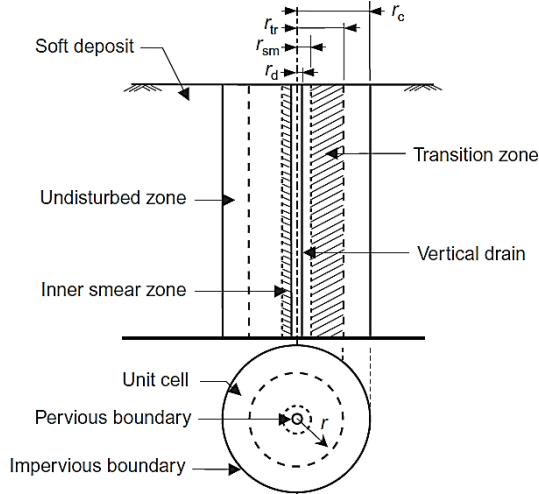


Figure 6 Separation of disturbed zone into inner smear zone and transition zone (Basu *et al.* 2010a)

The effect of soil disturbance is typically considered by assuming a constant value for the horizontal hydraulic conductivity  $k_x$  over the entire disturbed zone. The degree of soil disturbance  $\beta$  is defined in terms of the ratio  $k_s/k_h$ . Experimental investigations by Onoue *et al.* (1991), Madhav *et al.* (1993), Indraratna and Redana (1998b), Ghandeharion *et al.* (2012) and Rujikiatkamjorn *et al.* (2013) have shown that the horizontal hydraulic conductivity of soil in the disturbed zone is not spatially constant, but is a function of the normalised radial distance  $r/r_{m,eq}$  measured from the centre of the PVD, where  $r_{m,eq}$  ( $=\sqrt{A_m/\pi}$ ) is the equivalent radius of the mandrel and  $A_m$  is the cross-sectional area of the mandrel.

Over the past two to three decades, several researchers have performed analytical, laboratory, numerical and field studies to quantify the sources and effects of soil disturbance and well resistance on the behaviour of PVDs. This paper presents a review of these research efforts. The review is complemented by two case histories that highlight the performance of PVDs in the field.

## 2. ANALYTICAL STUDIES

For axisymmetric flow in a unit cell, the average degree of consolidation  $\bar{U}_h$  on a horizontal plane at depth  $z$  and time  $t$  can be predicted from (Hansbo 1981)

$$\bar{U}_h = 1 - \exp\left(-\frac{8T_h}{\mu}\right) \quad (5)$$

where  $T_h$  ( $=c_h t/4r_{c,eq}^2$ ) is the time factor for flow of pore water in the horizontal direction,  $c_h$  ( $=k_h/m_v\gamma_w$ ) is the horizontal coefficient of consolidation,  $m_v$  is the coefficient of volume compressibility,  $\gamma_w$  is the unit weight of water, and  $\mu$  is a parameter that accounts for PVD geometry and the effects of disturbance and well resistance.

Indraratna and Redana (1997) showed that the average degree of consolidation  $\bar{U}_{h,p}$  on a horizontal plane at depth  $z$  and time  $t$  in plane strain can be represented by

$$\bar{U}_{h,p} = 1 - \exp\left(-\frac{8T_{h,p}}{\mu_p}\right) \quad (6)$$

where  $T_{h,p} = (\mu_p/\mu)T_h$  is the time factor for horizontal flow in plane strain. Table 1 summarises different expressions for  $\mu$ ,  $\mu_p$  and other parameters proposed by various researchers based on analytical studies on PVD-improved ground. The table also shows the assumptions made in the derivation of these expressions and additional remarks. Three dimensionless terms,  $n$ ,  $m$  and  $q$ , are defined to normalise the radial distances from the centre of the PVD with respect to the equivalent radius of the PVD as  $n = r_{c,eq}/r_{d,eq}$ ,  $m = r_{sm}/r_{d,eq}$  and  $q = r_{tr}/r_{d,eq}$ . A brief discussion of the analytical studies is presented below.

Basu *et al.* (2006) and Basu *et al.* (2010a) developed closed-form analytical solutions for the rate of consolidation of PVD-improved ground considering four spatial profiles of horizontal hydraulic conductivity (denoted by Cases A, B, C and D in Table 1) under instantaneous and ramp preloading. These profiles consisted of either a constant or linearly varying horizontal hydraulic conductivity in the inner smear zone, and a linear or bilinear variation in the transition zone. Walker and Indraratna (2006), on the other hand, considered a parabolic variation of the horizontal hydraulic conductivity of soil in the disturbed zone. Thus, these studies indicate that proper identification of the horizontal hydraulic conductivity profile of soil around a PVD is necessary for accurate prediction of the rate of consolidation.

Indraratna *et al.* (2005) modified Hansbo's radial consolidation solution by: (1) replacing  $m_v$  with the compression and swelling indices,  $C_c$  and  $C_s$ , respectively, which define the slopes of the normal consolidation and recompression lines, respectively, in  $e$ - $\log\sigma'_v$  space;  $e$  is the void ratio and  $\sigma'_v$  is the vertical effective stress, and (2) considering the variation of  $k_h$  with  $e$  through the  $e$ - $\log k_h$  relationship that has a slope of  $C_k$  (the permeability index). Sathanathan and Indraratna (2006a) developed equivalent plane strain analytical solutions for both Darcian (linear) flow and non-Darcian (exponential) flow. Walker *et al.* (2012) combined the solutions of Indraratna *et al.* (2005) and Sathanathan and Indraratna (2006a), and developed a more rigorous non-linear, non-Darcian radial consolidation solution for PVD-improved ground subjected to instantaneous preloading. The ratio  $C_c/C_k$  or  $C_s/C_k$  and the loading increment ratio  $\Delta p_v/\sigma'_{v0}$  were found to influence the rate of consolidation of PVD-improved ground;  $\Delta p_v$  is the preload increment and  $\sigma'_{v0}$  is the initial vertical effective stress.

Walker and Indraratna (2007) investigated the effect of overlapping disturbed zones, caused by the installation of closely-spaced PVDs, on the rate of soil consolidation. The consolidation rate was found to be unaffected when the PVD spacing was reduced below a threshold value. This minimum influence radius was reported to be 0.6 times the value corresponding to a non-overlapping disturbed zone. Indraratna *et al.* (2008) developed an analytical solution for the rate of consolidation of PVD-improved ground subjected to instantaneous, circular loading, by substituting the discrete PVD system with a series of equivalent concentric cylindrical drain walls.

Ghandeharion *et al.* (2010) employed an elliptical cavity expansion theory in terms of Modified Cam-Clay (MCC) parameters to address the undrained analysis of PVDs installed in soft clay deposits. The ratio of the plastic shear strain to the rigidity index  $\gamma^p/I_r$  was used to identify the zones of disturbance around the PVD. The values of  $\gamma^p/I_r$  were found to range from 0.10–0.17% and 0.01–0.05% at the outer boundaries of the inner smear zone and the transition zone, respectively. However, there was no plastic shear strain and no change in pore pressure in the undisturbed elastic zone. Rujikiatkamjorn and Indraratna (2010) used a piecewise technique to analyse radial consolidation in a two-layered soil system considering the effect of soil downdrag caused by mandrel penetration, i.e., the effect of soil dragged down from the upper layer to create additional disturbance in the lower layer.

Table 1 Analytical Solutions for PVD-Improved Ground Response

Reference	Equation	Assumptions and remarks
Hansbo (1981)	$\mu = \ln\left(\frac{n}{q}\right) + \frac{1}{\beta} \ln(q) - \frac{3}{4} + \pi z(2l_d - z) \frac{k_h}{q_w}$	<ol style="list-style-type: none"> <li>1. Constant hydraulic conductivity in the disturbed zone</li> <li>2. Equal strain hypothesis with flow rate based on Darcy's law</li> </ol>
Indraratna and Redana (1997)	$\mu_p = c_1 + c_2 \frac{1}{\beta_p} + c_3(2l_d z - z^2); c_1 = \frac{2}{3} - \frac{2b_s}{b_c} \left(1 - \frac{b_s}{b_c} + \frac{b_s^2}{3b_c^2}\right)$ $c_2 = \frac{1}{b_c^2} (b_s - b_d)^2 + \frac{b_s}{3b_c^3} (3b_d^2 - b_s^2); c_3 = \frac{2k_{h,p}^2}{k_{s,p} b_c q_{w,p}} \left(1 - \frac{b_d}{b_c}\right); k_{h,p} = \frac{\mu_p}{\mu} k_h$	<ol style="list-style-type: none"> <li>1. Average degrees of consolidation for axisymmetric and plane strain conditions are equated</li> <li>2. Total width of unit cell in plane strain is equal to the PVD spacing</li> <li>3. <math>\mu</math> is estimated based on Hansbo (1981)</li> </ol>
Chai <i>et al.</i> (2001)	$k_{v,eq} = k_v \left[ 1 + \frac{0.625 \left(\frac{l_d}{r_{c,eq}}\right)^2 k_h}{\mu k_v} \right]$	<ol style="list-style-type: none"> <li>1. Equivalent vertical hydraulic conductivity <math>k_{v,eq}</math> of PVD-improved ground represents the effect of the vertical hydraulic conductivity of natural subsoil and the effect of radial drainage due to PVD</li> </ol>
Indraratna <i>et al.</i> (2005)	$e = e_0 - C_c \log\left(\frac{\sigma'_v}{\sigma'_{v0}}\right); e = e_0 + C_k \log\left(\frac{k_h}{k_{h0}}\right); T_h^* = 0.5 \left[ 1 + \left(1 + \frac{p_v}{\sigma'_{v0}}\right)^{1-(C_c/C_k)} \right] T_h; \text{ for NC soil}$	<ol style="list-style-type: none"> <li>1. Non-linear consolidation of PVD-improved ground via <math>e-\log\sigma'_v</math> and <math>e-\log k_h</math> relationships</li> <li>2. <math>\bar{U}_h</math> is estimated based on Hansbo (1981) but using modified time factor <math>T_h^*</math></li> <li>3. <math>\mu</math> is estimated based on Hansbo (1981) but neglecting well resistance</li> <li>4. <math>C_c</math> in the <math>T_h^*</math> equation is replaced by <math>C_s</math> for OC soil</li> </ol>
Basu <i>et al.</i> (2006) and Basu <i>et al.</i> (2010a)	<p>Case A: <math>\mu = \ln\left(\frac{n}{q}\right) + \frac{1}{\beta} \ln(m) + \frac{(q-m)}{(\beta q - m)} \ln\left(\frac{\beta q}{m}\right) - \frac{3}{4}</math></p> <p>Case B: <math>\mu = \ln\left(\frac{n}{q}\right) + \frac{(m-1)}{(\beta m - \beta_i)} \ln\left(\frac{\beta m}{\beta_i}\right) + \frac{(q-m)}{(\beta_i q - m)} \ln\left(\frac{\beta_i q}{m}\right) - \frac{3}{4}</math></p> <p>Case C: <math>\mu = \ln\left(\frac{n}{q}\right) + \frac{(q-1)}{(\beta q - 1)} \ln(\beta q) - \frac{3}{4}</math></p> <p>Case D: <math>\mu = \ln\left(\frac{n}{q}\right) + \frac{1}{\beta} \ln(m) + \frac{(j-m)}{(j\beta - \beta_j m)} \ln\left(\frac{j\beta}{\beta_j m}\right) + \frac{(q-j)}{(\beta_j q - j)} \ln\left(\frac{\beta_j q}{j}\right) - \frac{3}{4}</math></p>	<ol style="list-style-type: none"> <li>1. Case A: Constant <math>k_{sm}</math> in inner smear zone and linear variation of <math>k_{tr}</math> in transition zone</li> <li>2. Case B: Linear variations of <math>k_{sm}</math> and <math>k_{tr}</math> in inner smear zone and transition zone, respectively</li> <li>3. Case C: Linear variation of <math>k_s</math> throughout single disturbed zone</li> <li>4. Case D: Constant <math>k_{sm}</math> in inner smear zone and bilinear variation of <math>k_{tr}</math> in transition zone</li> <li>5. Degree of consolidation is calculated for both instantaneous and ramp preloading</li> <li>6. Consolidation achieved through vertical flow, and well resistance, are neglected</li> </ol>
Sathanathan and Indraratna (2006a)	$v = ki^{n_i} \text{ for } i \leq i_t; \text{ and } v = kn_i i_t^{n_i-1} (i - i_0) \text{ for } i \geq i_t; \text{ where } i_t = \frac{i_0 n_i}{n_i - 1}$	<ol style="list-style-type: none"> <li>1. Extension of Indraratna and Redana (1997) to incorporate a non-Darcian (power law) flow model based on Hansbo (1960)</li> </ol>
Walker and Indraratna (2006)	$\mu = \ln\left(\frac{n}{q}\right) + \frac{(q-1)^2}{(\beta q^2 - 2q + 1)} \ln(q\sqrt{\beta}) - \frac{q(q-1)\sqrt{1-\beta}}{2(\beta q^2 - 2q + 1)} \ln\left(\frac{1+\sqrt{1-\beta}}{1-\sqrt{1-\beta}}\right) - \frac{3}{4} + \pi z(2l_d - z) \frac{k_h}{q_w}$	<ol style="list-style-type: none"> <li>1. Parabolic variation of <math>k_s</math> throughout single disturbed zone</li> <li>2. <math>c_h</math> is assumed to be constant and Darcy's law is valid</li> </ol>
Walker and Indraratna (2007)	$\bar{U}_h = 1 - \exp\left(-\frac{8T_h}{\mu_{m_v} \mu}\right); \mu_{m_v} = 1 + \left(\frac{m_{v,s}}{m_v} - 1\right) \frac{(q-1)(q+2)}{3(n^2 - 1)}$	<ol style="list-style-type: none"> <li>1. Linear variations of <math>k_s</math> and <math>m_v</math> throughout single disturbed zone</li> <li>2. Equation for <math>\mu</math> is same as that of Case C of Basu <i>et al.</i> (2006) and Basu <i>et al.</i> (2010a)</li> </ol>
Bellezza and Fentini (2008)	$n = \left(\frac{\lambda}{A}\right)^B; \lambda = \frac{c_h t}{\ln(1 - \bar{U}_h)^{-1} r_{d,eq}^2}; A = \frac{\exp(-3.45g_c)}{2g_c}; B = (2 + g_c)^{-1}$	<ol style="list-style-type: none"> <li>1. <math>n</math> is expressed as an explicit function of degree of consolidation, time, drain size, and smear and well resistance parameters</li> <li>2. Design equation is based on the solution of Hansbo (1981)</li> </ol>

$$g_c = \left[ \left( \frac{1}{\beta} - 1 \right) \ln(q) + \frac{2}{3} \frac{\pi k_h l_d^2}{q_w} + 2.7 \right]^{-1}$$

Indraratna *et al.*  
(2008)

$$\mu_{ring} \approx \frac{2}{3} \alpha^2; \alpha = \frac{s}{r_{c,eq}}; k_{h,ring} = \frac{\mu_{ring}}{\mu} k_h$$

1. Discrete PVD system is converted into continuous concentric rings of equivalent drain walls
2.  $\mu$  is estimated based on Hansbo (1981) but neglecting well resistance

Abuel-Naga *et al.*  
(2012)

$$\mu = \ln(n) + \left[ \frac{1}{\beta} \frac{\ln(m)}{\ln(q)} + \frac{q-m}{(\beta q - m) \ln(q)} \ln\left(\frac{\beta q}{m}\right) - 1 \right] \ln(q) - \frac{3}{4}; \text{ for } n > 5$$

$$k_{s,eq} = \frac{k_h}{\frac{1}{\beta} \frac{\ln(m)}{\ln(q)} + \frac{q-m}{(\beta q - m) \ln(q)} \ln\left(\frac{\beta q}{m}\right)}$$

1. Idealized unit cell considers constant  $k_{sm}$  in inner smear zone and linear variation of  $k_{tr}$  in transition zone
2. Proposed equivalent unit cell replaces both the inner smear zone and the transition zone of the idealized unit cell by a single combined disturbed zone with equivalent horizontal hydraulic conductivity  $k_{s,eq}$
3. Radial flow rate and excess pore pressure in the idealized and proposed equivalent unit cells are equated. Well resistance is neglected

Deng *et al.* (2013)

$$q_w = q_{w0} \exp(-a_w t)$$

1. Exponential decay of PVD discharge capacity with time
2.  $q_{w0}$  is the initial discharge capacity of PVD and  $a_w$  is a decay coefficient that represents the rate of degradation of PVD discharge capacity

Abuel-Naga *et al.*  
(2015)

$$c_h = c_{h,i} \left[ 1 + \left( \frac{c_{h,f} - c_{h,i}}{c_{h,i}} \right) \left( \frac{\bar{U}_h}{100} \right) \right]$$

1.  $c_h$  is not constant but changes linearly with  $\Delta\sigma'_v$  from an initial value  $c_{h,i}$  to a final value  $c_{h,f}$  within the consolidation stress increment
2.  $\bar{U}_h$  is solved using an FE solver, FlexPDE, for ramp preloading

Note:  $\beta_p = k_{s,p}/k_{h,p}$ ,  $k_{s,p}$  = horizontal hydraulic conductivity of soil in disturbed zone for plane strain condition,  $k_{h,p}$  = *in situ* horizontal hydraulic conductivity of soil for plane strain condition, NC = normally consolidated, OC = overconsolidated,  $k_{h0}$  = initial horizontal hydraulic conductivity,  $\beta = k_s/k_h$ ,  $k_s$  = horizontal hydraulic conductivity of soil at drain–soil interface,  $\beta_t = k_t/k_h$ ,  $k_t$  = horizontal hydraulic conductivity of soil at the boundary between inner smear zone and transition zone,  $r_j$  = radial distance at which the bilinear profile of horizontal hydraulic conductivity within the transition zone changes slope,  $\beta_j = k_j/k_h$ ,  $k_j$  = horizontal hydraulic conductivity of soil within transition zone where the bilinear profile changes slope,  $i_l$  = limiting hydraulic gradient,  $i_0$  = threshold hydraulic gradient,  $n_i$  = power law parameter, and  $m_{v,s}$  = coefficient of volume compressibility of soil at drain–soil interface

Rujikiatkamjorn and Indraratna (2015) examined the effectiveness of non-traditional drain installation patterns, such as circular drain ring and parallel drain wall patterns, versus conventional (square or triangular) drain installation patterns, on the rate of soil consolidation. The time required to achieve 90% degree of consolidation at 1 m drain spacing was 14, 60 and 250 days for drain rings, drain walls, and the conventional square pattern, respectively. Lu *et al.* (2015) extended the non-linear radial consolidation solution of Indraratna *et al.* (2005) to analyse the rate of consolidation of PVD-improved ground subjected to multistage loading and preloading–unloading–reloading schemes. Lu *et al.* (2016) included multiple PVDs inside a unit cell and developed analytical solutions for four loading schemes: (1) instantaneous loading, (2) ramp loading, (3) multi-stage instantaneous loading, and (4) multi-stage ramp loading (Lei *et al.* 2015), considering the effects of soil disturbance, i.e., constant horizontal hydraulic conductivity in the disturbed zone, and well resistance of all the PVDs.

Huang *et al.* (2016) modelled the PVD as an elliptical cylindrical drainage body and obtained analytical solutions for excess pore pressure and degree of consolidation corresponding to an elliptical cylindrical coordinate system. Based on scientific evidence from microbiological studies, Indraratna *et al.* (2016) proposed an analytical solution for soil consolidation considering the degradation of natural fibre drains over time. An exponential form of reduction in drain discharge capacity was incorporated in the analysis (Deng *et al.* 2013). The dissipation of excess pore pressure got delayed significantly due to drain degradation, which depended on the magnitude of the decay coefficient.

### 3. LABORATORY STUDIES

Table 2 summarises the results of 10 laboratory studies on PVD-treated soft clay performed by various researchers. The table displays information about the type of laboratory test, size of soil sample inside the test chamber, soil type and properties, details of the PVD used, test parameters, and important observations. The information tabulated in Table 2 is helpful to researchers formulating a laboratory PVD testing program. A brief discussion of the laboratory studies is presented below.

Based on the results obtained from discharge capacity tests, Chu *et al.* (2006) reported an 84% reduction in PVD discharge capacity after the PVD had experienced a vertical compressive strain of 46%. Fang and Yin (2006) observed buckling of the PVD, particularly in the upper section, after the PVD had experienced a vertical compressive strain of 15%. The buckled PVD did not fully dissipate the excess pore pressures in Hong Kong marine clay at the end of the loading period. Similarly, Tran-Nguyen *et al.* (2010) reported a 90–99.5% reduction in PVD discharge capacity corresponding to a vertical compressive strain of 40%. Thus, these studies indicate that the discharge capacity of a PVD can decrease substantially after the PVD has experienced large deformations.

Shin *et al.* (2009) performed a series of radial penetration tests, using a 5-mm-diameter micro-cone penetrometer and a 2.1-mm-diameter electrical resistance probe, to evaluate the radius of the disturbed zone caused by the installation of a PVD with a rectangular mandrel into reconstituted Busan clay. The shape of the disturbed zone was found to be elliptical and not circular. The radius  $r_s$  of the disturbed zone was equal to 4.0 to 4.2 times  $r_{m,eq}$  along the direction of the mandrel's longer axis and 3.3 to 3.4 times  $r_{m,eq}$  along the direction of the mandrel's shorter axis. Based on a series of large-scale, sinusoidal, cyclic triaxial tests on soft kaolinite clay, with and without the inclusion of PVD, Indraratna *et al.* (2009) showed that PVD-treated soft clay can sustain cyclic stress levels higher than the critical cyclic stress ratio (CSR) without undergoing undrained shear failure. Moreover, the PVD significantly reduced the buildup of excess pore pressure in soft clay during cyclic loading, and accelerated its dissipation after the load was removed.

Howell *et al.* (2012) performed dynamic centrifuge tests at a centrifugal acceleration of 15g to evaluate the performance of liquefiable soil treated with 40 PVDs spaced at 1.5 m (prototype scale) in a triangular pattern. The centrifuge model consisted of 370-mm-thick, loose ( $D_R = 40\%$ ) Nevada sand overlain by a 100-mm-thick layer of Yolo loam clay (Howell *et al.* 2009), sloping downwards at an angle of  $10^\circ$  with the horizontal. The circular, wished-in-place PVDs had an inner diameter of 6.35 mm and were perforated with 1.5-mm-diameter holes spaced at 7.6 mm in a staggered pattern. Nine shaking events were applied to the model over a period of 5.5 hours. Scaled earthquake input motions, ranging in peak ground acceleration (PGA) from 0.11–0.95g, were used for the first 8 shaking events, and a sine wave with 20 cycles of motion at frequency of 2 Hz and PGA of 0.6g was used for the final shaking event. The reductions in lateral deformation and settlement of PVD-improved Nevada sand were of the order of 30–60% and 20–60%, respectively, with maximum reduction occurring under the most intense shaking event.

Based on the results obtained from large-scale consolidation tests on PVD-improved Bangkok clay, Saowapakpiboon *et al.* (2010) determined the values of  $r_s/r_{m,eq}$  and  $k_s/k_h$  to be 2 and 0.37, respectively. Ghandeharioon *et al.* (2012), Rujikiatkamjorn *et al.* (2013) and Sengul *et al.* (2016) measured the values of  $r_{sm}/r_{m,eq}$  and  $r_{tr}/r_{m,eq}$  to be 2.65 and 5.8 for reconstituted kaolin clay, 3.7 and 5.5 for undisturbed lacustrine clay, and 3.3 and 7.3 for reconstituted kaolin clay, respectively. Rujikiatkamjorn *et al.* (2013) reported the values of  $k_{sm}/k_h$  and  $k_{tr}/k_h$  to range from 0.35–0.75 and 0.75–0.90, respectively, whereas Sengul *et al.* (2016) reported them to be equal to 0.50 and 0.82, respectively. The methods used for the determination of these parameters are described in Section 3.1.

Chai and Xu (2015) performed laboratory model tests to investigate the effect of the surcharge loading rate on the magnitude of lateral displacement  $\delta$  of PVD-improved Ariake clay. The maximum lateral displacement  $\delta_{max}$  was observed to increase from 10 to 26 mm with increase in loading rate from 2 to 7 kPa/day. Asha and Mandal (2015) proposed discharge capacity reduction factors  $q_{w,RF}$ , defined as the ratio of the discharge capacity of a PVD confined in marine clay to the discharge capacity of a PVD confined in a rubber membrane, ranging from 0.4–0.5 for natural (jute) PVDs and equal to 0.6 for polymer-based PVD. Deng *et al.* (2017) reported that the degree of consolidation of PVD-improved grey clay was 20% greater than that of unimproved clay after a loading period of 4 weeks.

#### 3.1 Measured Degrees of Soil Disturbance and Radii of Disturbed Zone, Inner Smear Zone and Transition Zone

The degrees of soil disturbance, expressed in terms of the hydraulic conductivity ratios  $k_s/k_h$ ,  $k_{sm}/k_h$  and  $k_{tr}/k_h$ , and the normalised radii of the disturbed zone  $r_s/r_{m,eq}$ , inner smear zone  $r_{sm}/r_{m,eq}$  and transition zone  $r_{tr}/r_{m,eq}$ , measured from 13 experimental studies, are quantified in Table 3. These parameters are typically measured in the laboratory by coring soil specimens, horizontally and vertically, from known radial distances and vertical depths around the PVD (Figure 7), and subsequently performing water content and oedometer tests on those specimens (Indraratna and Redana 1998a,b; Sathananthan and Indraratna 2006b; Ghandeharioon *et al.* 2012; Rujikiatkamjorn *et al.* 2013). The specimens are extracted from a large-scale consolidometer either immediately after the dissipation of excess pore pressures generated due to the insertion of the mandrel (Sharma and Xiao 2000), or after completion of primary consolidation of PVD-improved soil under the applied preload (Indraratna and Redana 1998a,b; Sathananthan and Indraratna 2006b; Ghandeharioon *et al.* 2012; Rujikiatkamjorn *et al.* 2013; Deng *et al.* 2017). An alternate approach to measure the spatial variation of the horizontal hydraulic conductivity is to directly perform hydraulic conductivity tests on PVD-improved soil (Hird and Moseley 2000; Sengul *et al.* 2016).

Table 2 Laboratory Studies on Reconstituted and Undisturbed Soft Clay Specimens Improved with PVD

Reference	Type of test	Sample size	Soil type and properties	PVD details	Loading details	Observations
Chu <i>et al.</i> (2006)	LC	$d = 495$ mm $h/d = 1.52$	Clay+silt mixture from slurry pond $w_L = 65\text{--}115\%$ , $PI = 43\text{--}70\%$ $w_c = 75\text{--}180\%$ , $e = 2.0\text{--}4.5$	Colbond drain CX1000 $b_w = 100$ mm, $b_t = 5.3$ mm $q_w = 2207.5$ m <sup>3</sup> /yr, $O_{95} < 0.07$ mm	$p_v = 110$ kPa	$w_{max} = 340$ mm after 130 days $\Delta q_w = 84\%$ (reduction)
Fang and Yin (2006)	LC	$d = 300$ mm $h/d = 0.67$	Reconstituted Hong Kong marine clay $w_L = 51.1\%$ , $PI = 25\%$ , $w_c = 1.7w_L$	Colbond drain CX1000 $b_w = 50$ mm, $b_t = 5$ mm	$p_v = 80$ kPa in 4 stages	$w_{max} = 30$ mm at 187 days, $\bar{u}_{max} = 21$ kPa
Indraratna <i>et al.</i> (2009)	Cyclic CK <sub>0</sub> U and CK <sub>0</sub> D	$d = 300$ mm $h/d = 2.0$	Reconstituted kaolin clay $w_L = 55\%$ , $PI = 28\%$ , $w_c = 1.1w_L$ $e = 1.46$ , $C_c = 0.42$ , $C_s = 0.06$	Mebra drain MD88 $b_w = 32$ mm, $b_t = 4$ mm $q_w > 150$ m <sup>3</sup> /yr	$\sigma'_v = 40$ kPa ( $K_0 = 0.6$ ) $f = 5$ Hz, $a = 25$ kPa $CSR = 0.65$	For 400 loading cycles No PVD: $\varepsilon_a = 11.1\%$ , $R_u = 0.85$ With PVD: $\varepsilon_a = 2.8\%$ , $R_u = 0.13$
Saowapakpiboon <i>et al.</i> (2010)	LC	$d = 305$ mm $h/d = 1.64$	Reconstituted Bangkok clay $w_L = 102.2\%$ , $PI = 62.7\%$ , $w_c = 1.1w_L$	CeTeau drain CT-D911 $b_w = 100$ mm, $b_t = 3.5$ mm	$p_v = 100$ kPa	$w_{max} = 23$ mm after 24 days $r_s/r_{m,eq} = 2$ , $k_s/k_h = 0.37$
Ghandeharion <i>et al.</i> (2012)	LC	$d = 650$ mm $h/d = 1.38$	Reconstituted kaolin clay $w_L = 55\%$ , $PI = 28\%$ , $w_c = 1.1w_L$	$b_w = 100$ mm $b_t = 4$ mm	$p_v = 50$ kPa	$r_{sm}/r_{m,eq} = 2.65$ , $r_{tr}/r_{m,eq} = 5.8$ $(k_{tr}/k_v)_{sm} = 1.2\text{--}1.6$ , $(k_{tr}/k_v)_{tr} = 1.6\text{--}1.8$
Rujikiatkamjorn <i>et al.</i> (2013)	LC	$d = 345$ mm $h/d = 1.63$	Undisturbed lacustrine clay $w_L = 50\%$ , $PI = 25\%$ , $w_c = 0.83w_L$ $e = 1.13$ , $\sigma'_{vp} = 80$ kPa, $OCR = 2.5$	NW geotextile filter $b_w = 50$ mm $b_t = 5$ mm	$p_v = 200$ kPa in 4 stages	$w_{max} = 28$ mm after 31 days $r_{sm}/r_{m,eq} = 3.7$ , $r_{tr}/r_{m,eq} = 5.5$ $k_{sm}/k_h = 0.35\text{--}0.75$ , $k_{tr}/k_h = 0.75\text{--}0.90$
Asha and Mandal (2015)	DC and LC	DC: $200 \times 100 \times 50$ mm LC: $d = 480$ mm $h/d = 1.25$	Reconstituted marine clay $w_L = 82\%$ , $PI = 42\%$ $w_c = 1.04w_L$ and $1.3w_L$ $e = 2.72\text{--}2.80$ , $C_c = 0.75$	Woven-jute, NW-jute, and NW-PP filters, $b_w = 85\text{--}100$ mm $b_t = 5.0\text{--}16.5$ mm $O_{95} = 0.075\text{--}0.25$ mm	DC: $\sigma_c = 10\text{--}250$ kPa $i = 0.1\text{--}1.0$ LC: $p_v = 150$ kPa in 4 stages	$w = 194$ mm after 93 days (no PVD) and 45 days (with NW-PP PVD) $q_{w,RF} = 0.4\text{--}0.5$ (for natural drains) and 0.6 (for polymer-based drain)
Chai and Xu (2015)	LC	$1500 \times 600 \times 800$ mm	Reconstituted Ariake clay $w_L = 114\%$ , $PI = 53.4\%$ $w_c = 1.1w_L$ and $1.3w_L$	NW geotextile filter $b_w = 30$ mm, $b_t = 10$ mm $s_x = 166$ mm, $s_y = 150$ mm	$p_v = 60$ kPa @ 2–7 kPa/day	$w_{max} = 80\text{--}105$ mm after 25 days $\delta_{max} = 10\text{--}26$ mm at 15–25 mm depth $\bar{u}_{max} = 8$ kPa
Sengul <i>et al.</i> (2016)	SZM	$350 \times 130 \times 500$ mm	Reconstituted kaolin clay $w_L = 51\%$ , $PI = 25\%$ , $w_c = 1.06w_L$ $e = 1.51$ , $C_c = 0.25$	$b_w = 100$ mm, $b_t = 3.6$ mm $q_w = 4225.8$ m <sup>3</sup> /yr $O_{95} = 0.14$ mm	$p_v = 50$ kPa	$r_{sm}/r_{m,eq} = 3.3$ , $r_{tr}/r_{m,eq} = 7.3$ $k_{sm}/k_h = 0.50$ , $k_{tr}/k_h = 0.82$
Deng <i>et al.</i> (2017)	LC	$d = 500$ mm $h/d = 2.1$	Reconstituted grey clay $w_L = 47\%$ , $PI = 23\%$ $w_c = 1.06w_L$ , $e = 1.25$ , $C_c = 0.27$	$b_w = 100$ mm $b_t = 4$ mm $q_w > 500$ m <sup>3</sup> /yr	$p_v = 100$ kPa in 4 stages	$w = 54$ mm (no PVD) and 72 mm (with PVD) after 28 days, $\bar{u}_{max} = 42$ kPa (no PVD) and 24 kPa (with PVD)

Note: DC = discharge capacity, LC = large-scale consolidation, SZM = smear zone model, CK<sub>0</sub>U and CK<sub>0</sub>D =  $K_0$ -consolidated undrained and partially drained triaxial tests,  $w_c$  = water content of soil sample inside the test chamber, NW = non-woven, PP = polypropylene,  $w_{max}$  = maximum surface settlement,  $\delta_{max}$  = maximum lateral displacement, and  $\bar{u}_{max}$  = maximum average excess pore pressure

Table 3 Measured Degrees of Soil Disturbance and Radii of Disturbed Zone, Inner Smear Zone and Transition Zone

Reference	Disturbed zone		Inner smear zone		Transition zone	
	$k_s/k_h$	$r_s/r_{m,eq}$	$k_{sm}/k_h$	$r_{sm}/r_{m,eq}$	$k_{tr}/k_h$	$r_{tr}/r_{m,eq}$
Hansbo (1986)	0.33	2	—	—	—	—
Bergado <i>et al.</i> (1991)	0.50–0.67	2	—	—	—	—
Onoue <i>et al.</i> (1991)	0.2–0.6	6–7	0.2–0.5	3	0.5–0.6	6–7
Bergado <i>et al.</i> (1993b)	0.5	2	—	—	—	—
Madhav <i>et al.</i> (1993)	0.2–1.0	10.3	0.2	1.5	0.2–1.0	10.3
Hird and Moseley (2000)	0.33	2–3	—	—	—	—
Sharma and Xiao (2000)	0.77	4	—	—	—	—
Sathanathan and Indraratna (2006b) and Sathanathan <i>et al.</i> (2008)	0.61–0.92	2.5	—	—	—	—
Saowapakpiboon <i>et al.</i> (2010)	0.37	2	—	—	—	—
Rujikiatkamjorn <i>et al.</i> (2013)	0.35–0.90	5.5	0.35–0.75	3.7	0.75–0.90	5.5
Indraratna <i>et al.</i> (2015)	0.2–1.0	6.3	—	—	—	—
Sengul <i>et al.</i> (2016)	0.32–0.57	5.2–5.8	0.32	2.3–2.4	0.57	5.2–5.8

Note: The disturbed zone consists of both the inner smear zone and the transition zone (Figure 6)

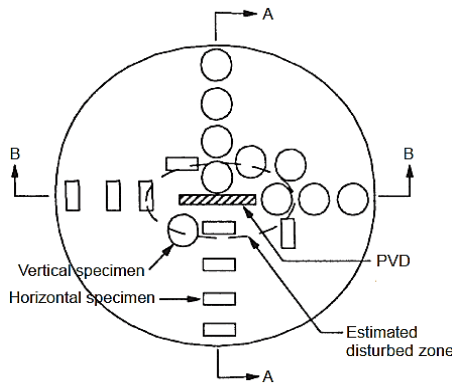


Figure 7 General illustration of horizontal and vertical sampling locations (in plan) for water content and oedometer testing (modified from Indraratna and Redana 1998b)

The installation rate of the mandrel in laboratory tests typically varies from 0.5 to 20 mm/s (Hird and Moseley 2000; Sharma and Xiao 2000; Sathanathan and Indraratna 2006b; Sengul *et al.* 2016). However, Ghandeharion *et al.* (2012) employed a much higher mandrel installation rate of 100 mm/s in their laboratory tests. It should be noted that the data reported by Madhav *et al.* (1993) and Indraratna *et al.* (2015) in Table 3 are based on samples collected from different radial distances from an *in situ* soil into which a PVD was installed. Referring to Table 3, the hydraulic conductivity  $k_{sm}$  of soil in the inner smear zone, adjacent to the PVD, reduces to about 0.20 to 0.35 times the hydraulic conductivity  $k_h$  of soil in the undisturbed zone, increases gradually with radial distance in the transition zone, and finally approaches the value of  $k_h$  at the boundary between the transition zone and the undisturbed zone. Based on the data listed in Table 3, the radius  $r_{sm}$  of the inner smear zone varies from 1.5 to 3.7 times the equivalent radius  $r_{m,eq}$  of the mandrel, whereas the radius  $r_{tr}$  of the transition zone varies from 5.2 to 10.3 times  $r_{m,eq}$  depending on the type of soil and the size and installation rate of the mandrel. In the absence of test data, Chai and Miura (1999) suggest that the radius  $r_s$  of the entire disturbed zone may be taken as 3 times  $r_{m,eq}$ .

#### 4. NUMERICAL STUDIES

Table 4 summarises 10 numerical studies on PVD-improved ground performed by various researchers. The table displays information about the numerical code and software used, type of analysis, constitutive model for soft ground, PVD parameters, type of mesh element, and loading details. It should be noted that all the numerical studies listed in Table 4 considered the smear zone to be a single disturbed zone with radius  $r_s$  and hydraulic conductivity  $k_s$ , i.e., the disturbed zone was not subdivided into the inner smear zone

and the transition zone. The values of  $k_s/k_h$  reported in Table 4 have been used in numerical simulations by researchers to predict deformations and excess pore pressures of PVD-improved ground. These predictions have subsequently been validated against field measurements; in other words, the values of  $k_s/k_h$  reported in Table 4 were assumed to be representative of the field values. However, these values are smaller than the values of  $k_s/k_h$  measured in the laboratory (Table 3) because: (1) PVDs are installed at much higher rates in the field (up to 1.5 m/s) (Indraratna *et al.* 2015) than in the laboratory (0.5 to 20 mm/s), (2) *in situ* soil is subjected to more shearing due to the greater length of the PVDs installed in the field (Indraratna *et al.* 2015), (3) soft clay deposits in the field are not uniform and may contain thin sand seams and lenses, which are difficult to replicate in the laboratory (Chai and Miura 1999), and (4) the effects of non-uniform consolidation (Zhou and Chai 2017).

Chai and Miura (1999) proposed an expression to estimate the field hydraulic conductivity ratio  $(k_s/k_h)_f$  in terms of the laboratory hydraulic conductivity ratio  $(k_s/k_h)_l$  as

$$\left(\frac{k_s}{k_h}\right)_f = \frac{1}{C_f} \left(\frac{k_s}{k_h}\right)_l \quad (7)$$

where subscripts  $f$  and  $l$  refer to the field and the laboratory, respectively, and  $C_f$  is the hydraulic conductivity ratio between field and laboratory values. According to Chai and Miura (1999), the value of  $C_f$  is sensitive to site stratigraphy, i.e.,  $C_f$  is close to 1 for a homogeneous deposit, but is greater than 1 for stratified deposits that contain thin sand layers and sand lenses. The value of  $C_f$  for most clay deposits varies from 2 to 25 depending on the type and origin of the clay (Chai and Miura 1999).

Among the numerical studies listed in Table 4, the finite element method (FEM) was used more often than the finite difference method (FDM) for the simulation of PVD-improved ground. The work done includes axisymmetric unit cell, equivalent plane strain and complex three-dimensional (3D) analyses. Several constitutive models were used to capture the elasto-plastic response of soft ground; the Modified Cam-Clay (MCC) (Roscoe and Burland 1968) and Soft Soil (SS) models were most commonly used. The SS model is based on the MCC model and is commercially available in the FE analysis program PLAXIS. The SS model assumes a logarithmic relationship between volumetric strain  $\epsilon_v$  (instead of void ratio  $e$  in the MCC model) and mean effective stress  $p'$ . However, the parameter  $M$  in the yield function of the SS model is not the slope of the critical state line (as in the MCC model), and is calculated from the coefficient of lateral earth pressure at-rest  $K_0^{nc}$  (instead of the angle of shearing resistance  $\phi$  in the MCC model). Material failure in the SS model is governed by the Mohr-Coulomb yield criterion with strength parameters  $c$  and  $\phi$ .

Table 4 Numerical Simulations on PVD-Improved Ground

Reference	Numerical code	Type of analysis	Constitutive model for soft ground	PVD parameters	Discretization of domain	Loading
Indraratna and Redana (2000)	FEM (CRISP92)	Plane Strain	Modified Cam-Clay model	$b_w = 105 \text{ mm}$ , $b_t = 4 \text{ mm}$ $s = 1.3 \text{ m}$ (triangular), $r_s/r_{m,eq} = 2.6$ $k_s/k_h = 0.04$ , $q_w = 40 \text{ m}^3/\text{year}$	8-noded linear strain quadrilateral elements with pore pressure nodes at corners	$p_v = 97.2 \text{ kPa}$ in 2 stages
Arulrajah <i>et al.</i> (2005)	FEM (PLAXIS)	Axisymmetric and Plane Strain	Soft Soil model	$s = 2, 2.5, 3 \text{ m}$ (square) $k_{eq}/k_h = 0.72$ (axisymmetric) $k_s/k_h = 0.13$ (plane strain)	6-noded triangular elements	$p_v = 51 \text{ kPa}$
Tarefder <i>et al.</i> (2009)	FEM (SAGE CRISP)	Plane Strain	Modified Cam-Clay model	$s = 1 \text{ m}$ (triangular) $r_s/r_{d,eq} = 2.5$ , $r_{c,eq}/r_{d,eq} = 20$ $k_s/k_h = 0.1$	8-noded linear strain quadrilateral elements with pore pressure nodes at corners	$p_v = 45 \text{ kPa}$ in 4 stages
Lin and Chang (2009)	FDM (FLAC)	3D	Modified Cam-Clay model	$b_w = 100 \text{ mm}$ , $b_t = 4 \text{ mm}$ , $s = 1.5 \text{ m}$ (square) $r_s/r_{m,eq} = 2$ , $r_s/r_{d,eq} = 3.2$ $r_{c,eq}/r_{d,eq} = 32.6$ , $k_s/k_h = 0.13$ $k_{eq}/k_h = 0.3$ , $q_w = 65 \text{ m}^3/\text{year}$	Quadrilateral block elements	$p_v = 75.6 \text{ kPa}$ in 5 stages
Lam <i>et al.</i> (2015)	FEM (ABAQUS)	Axisymmetric	Modified Cam-Clay model	$b_w = 100 \text{ mm}$ , $b_t = 3 \text{ mm}$ , $s = 1 \text{ m}$ (square) $r_s/r_{m,eq} = 2$ , $r_s/r_{d,eq} = 3.7$ , $r_{c,eq}/r_{d,eq} = 21.9$ $k_s/k_h = 0.10-0.17$	CAX8RP 8-noded biquadratic displacement, bilinear pore pressure elements	$p_v = 68.4 \text{ kPa}$ in 4 stages
Liu and Rowe (2015)	FEM (ABAQUS)	3D	Drucker-Prager model with elliptical yield cap	$b_w = 100 \text{ mm}$ , $b_t = 4 \text{ mm}$ $s = 2 \text{ m}$ (square), $k_s/k_h = 0.33$ $q_w = 120 \text{ m}^3/\text{year}$	C3D8P 8-noded linear displacement brick elements with linear pore pressures	$p_v = 110 \text{ kPa}$ in 11 stages
Oliveira <i>et al.</i> (2015)	FEM	Plane Strain and 3D	Modified Cam-Clay model	$b_w = 100 \text{ mm}$ , $b_t = 3 \text{ mm}$ $s = 2.2 \text{ m}$ (square), $r_s/r_{d,eq} = 5$ $k_s/k_h = 0.5$ , $q_w = 790 \text{ m}^3/\text{year}$	8 and 20-noded isoparametric quadrilateral elements	$p_v = 178.2 \text{ kPa}$ in 6 stages
Yildiz and Uysal (2015)	FEM (PLAXIS 2D)	Plane Strain	Modified Cam-Clay model, Soft Soil Creep model and Anisotropic Creep model	$b_w = 100 \text{ mm}$ , $b_t = 4 \text{ mm}$ $s = 1 \text{ m}$ (square), $r_s/r_{m,eq} = 5$ $k_s/k_h = 0.05$	6-noded triangular elements	$p_v = 60.9 \text{ kPa}$ in 6 stages
Chen <i>et al.</i> (2016a)	FEM (PLAXIS 3D)	3D	Hardening Soil model (isotropic hardening)	$s = 1.5 \text{ m}$ (triangular), $r_s/r_{m,eq} = 1.1$ and 3 $k_{eq}/k_h = 0.1$ and 0.3	10-noded tetrahedral elements	$p_v = 144.4 \text{ kPa}$ in 10 stages
Chen <i>et al.</i> (2016b)	FEM	Plane Strain	Soft Soil model	$b_w = 100 \text{ mm}$ , $b_t = 4 \text{ mm}$ , $s = 1.5 \text{ m}$ (triangular), $r_s/r_{m,eq} = 3$ , $r_s/r_{d,eq} = 6.8$ $r_{c,eq}/r_{d,eq} = 30.3$ , $k_s/k_h = 0.07$ , $q_w = 80 \text{ m}^3/\text{year}$	15-noded elements with 12 Gauss points	$p_v = 106 \text{ kPa}$ in 8 stages

Note:  $k_{eq} = f(k_s/k_h)$  is the equivalent hydraulic conductivity of PVD-improved ground

Furthermore, anisotropic behaviour and secondary consolidation (creep) of soft soil are not considered by the SS model. A brief discussion of the numerical studies listed in Table 4, as well as other related studies, is presented next.

Madhav *et al.* (1993) modelled PVD-treated ground as a 2D cartesian consolidation problem consisting of three distinct zones, namely, the inner smear zone consisting of highly remoulded soil, the transition zone consisting of marginally disturbed soil, and the undisturbed zone. The governing Terzaghi–Rendulic radial consolidation equation was solved by means of boundary and continuity conditions, in terms of the magnitude of the excess pore pressure  $u$  and the gradients of the excess pore pressure  $\partial u/\partial x$  and  $\partial u/\partial y$ , using FDM. The soil was assumed to be isotropic and its compressibility unaffected by disturbance. It was observed that the horizontal hydraulic conductivity and radius of the inner smear zone strongly influenced the consolidation rate rather than those of the transition zone. Instead of using closely-spaced PVDs, Madhav *et al.* (1993) suggest reducing the size of the mandrel or modifying the shape of the PVD to a circle or an ellipse to improve the response of PVD-treated ground.

Basu and Madhav (2000) extended the analysis of Madhav *et al.* (1993) to investigate the effect of PVD geotextile filter clogging on the consolidation rate. Four cases of PVD clogging were investigated: (A) clogging from the tip of the PVDs to the center, (B) clogging from the center of the PVDs to the tip, (C) clogging from the middle of each PVD half, and (D) discontinuous clogging (Figure 8). The effect of PVD clogging on the rate of soil consolidation was maximum for Case A when compared to cases B, C and D (Figure 9). For a time factor  $T_h$  of 1.0, the average degree of consolidation  $\bar{U}_h$  for Case A decreased from 95.2% (for no clogging) to 89.5% (for 50% PVD clogging) and further down to 73.3% (for 95% PVD clogging). Moreover, for 95% PVD clogging, the time required to reach 90% degree of consolidation was more than twice the time needed by an unclogged PVD. Because of PVD clogging, the spacing of the PVDs ( $s_x \times s_y = 1 \text{ m} \times 1 \text{ m}$ ,  $1.25 \text{ m} \times 1 \text{ m}$ ,  $1.5 \text{ m} \times 1 \text{ m}$ , and  $2 \text{ m} \times 1 \text{ m}$ ) did not have any significant effect on the consolidation rate.

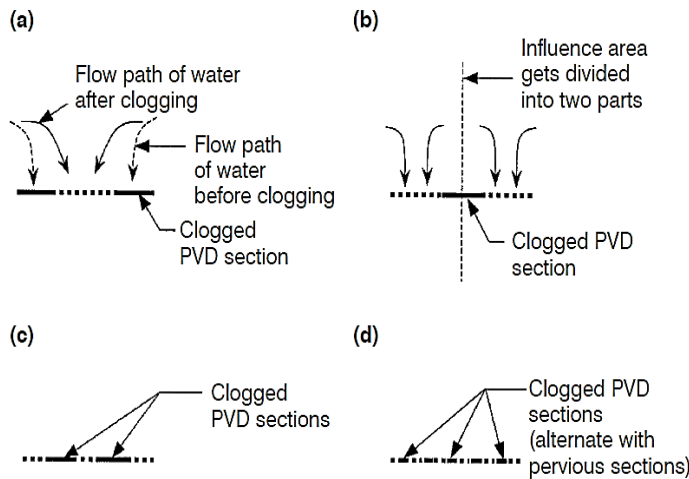


Figure 8 Methods of PVD clogging: (a) clogging from the tip of the PVD (Case A), (b) clogging from the center of the PVD (Case B), (c) clogging from the middle of each half of the PVD (Case C), and (d) discontinuous clogging (Case D) (Basu and Madhav 2000)

Basu and Prezzi (2007) and Basu and Prezzi (2008) performed 2D FE analyses of soil improved with PVDs installed in a triangular pattern considering the effect of soil disturbance. The horizontal hydraulic conductivity of soil was varied spatially according to Case A of Basu *et al.* (2006) described in Table 1. The actual hexagonal shape of the unit cell, band shape of the drain, and rectangular

shapes of the inner smear zone and the transition zone were used in the analyses, i.e., they were not converted into equivalent circles. The discretized version of the Terzaghi-Rendulic differential equation was solved using an implicit (backward difference) numerical time integration scheme, and three-noded triangular elements were used to discretize the domain. A method to replace the transition zone by an equivalent expanded disturbed zone was proposed. Basu *et al.* (2010b) extended these simulations for PVDs installed in a rectangular pattern and proposed a method for converting rectangular disturbed zones into equivalent circles.

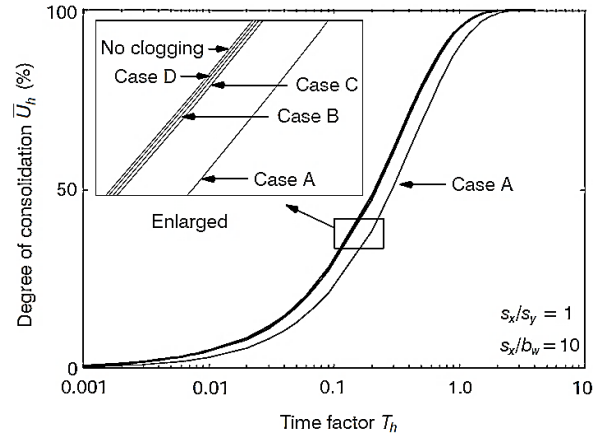


Figure 9 Average degree of consolidation  $\bar{U}_h$  vs. time factor  $T_h$  – effect of 50% PVD clogging for Cases A, B, C and D (modified from Basu and Madhav 2000)

Basu and Prezzi (2009), Basu and Prezzi (2010) and Basu *et al.* (2013) approximated the horizontal hydraulic conductivity profile of soil in the transition zone by a sigmoidal curve and performed 2D FE analyses for triangular and square PVD arrangements. The results obtained from their FE analyses matched reasonably well with those obtained from an analytical solution assuming a bilinear horizontal hydraulic conductivity profile in the transition zone. Based on the analytical solution, design charts were developed to obtain the PVD spacing for the desired degree of consolidation, considering also the overlapping of disturbed zones.

Tarefder *et al.* (2009) developed a 2D plane strain FE model to analyse consolidation and lateral displacement of soft Bangkok clay, with and without the inclusion of PVDs, under both embankment and vacuum preloading. The effect of soil disturbance was incorporated through the following expression for the horizontal hydraulic conductivity  $k_{h,p}$  of soil in plane strain

$$k_{h,p} = \frac{\pi L}{s_{row} \left[ \ln\left(\frac{n}{q}\right) + \frac{1}{\beta} \ln(q) \right]} k_h \quad (8)$$

where  $k_h$  is the *in situ* horizontal hydraulic conductivity of soil for axisymmetric condition,  $L$  is half the distance between the PVDs in plane strain,  $s_{row}$  is the *in situ* row spacing of the PVDs, and  $\beta = k_s/k_h$ . For a triangular PVD pattern,  $s_{row}$  is equal to  $(\sqrt{3}/2)s$ . The equivalent width  $b_d$  of the PVD in plane strain was calculated using the expression  $b_d = \pi r_{d,eq}^2 / s_{row}$  which is based on stiffness and loading equivalence between axisymmetric and plane strain conditions. The settlement of the embankment after 144 days with vacuum preloading was 75% greater than that without vacuum preloading, whereas the lateral deformation of Bangkok clay with vacuum was 64% of that without the use of vacuum. The undrained shear strength  $s_u$  of Bangkok clay increased by 60–80% within 0–6 m depth due to the use of PVDs. Abuel-Naga and Bouazza (2009)

numerically evaluated the equivalent radius of a PVD to be 0.2273 times the width of the PVD by using an equal flow rate approach.

Using FDM, Khan *et al.* (2010) analysed the problem of non-linear consolidation for radial flow around a PVD in a thick clay deposit, based on the non-linear theory of consolidation for vertical flow presented by Davis and Raymond (1965). The variation of the initial *in situ* stress with depth in a thick clay deposit was considered along with a linear void ratio–log effective stress relationship assuming a constant horizontal coefficient of consolidation. The normalised excess pore pressure  $u/u_0$ , estimated from the non-linear radial consolidation theory, was found to depend on both the normalised depth  $z/H$  as well as the surcharge parameter  $p_v^*$  ( $= p_v/\gamma_b H$ ) (Figure 10(a) and Figure 10(b)). In contrast, the conventional linear theory is independent of  $z/H$  and  $p_v^*$ , and thus underestimates the normalised excess pore pressure.

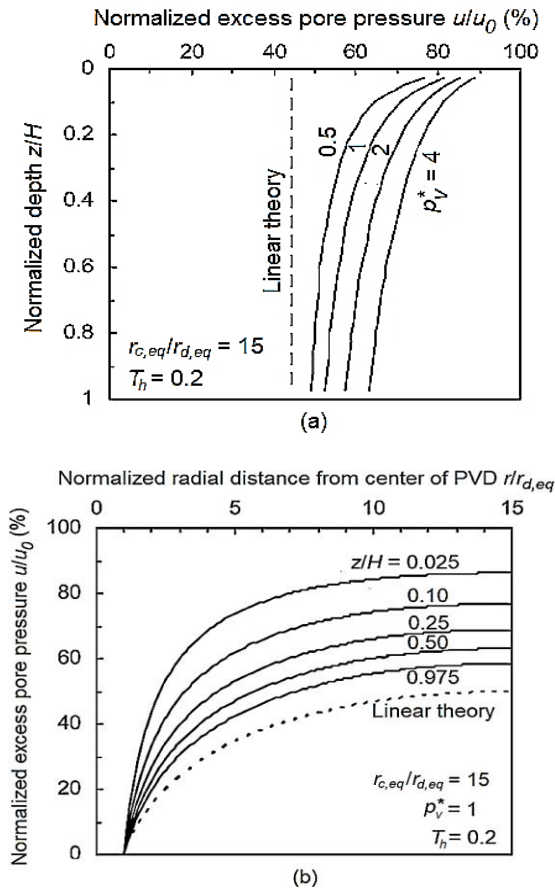


Figure 10 Non-linear thick layer consolidation of PVD-improved soil: (a)  $u/u_0$  vs.  $z/H$  – effect of  $p_v^*$ , and (b)  $u/u_0$  vs.  $r/r_{d,eq}$  – effect of  $z/H$  (modified from Khan *et al.* 2010)

Apart from axisymmetric and plane strain FE analyses, full-scale 3D numerical simulations of PVD-improved ground to support embankments (Lin and Chang 2009; Liu and Rowe 2015; Oliveira *et al.* 2015) and geogrid-reinforced soil wall (Chen *et al.* 2016a) have also been performed. Lin and Chang (2009) modelled band-shaped PVDs as equivalent cylindrical-shaped drainage channels with equivalent radius  $r_{d,eq}$  estimated from Eq. (4). The effect of soil disturbance was incorporated through the following expression for the equivalent hydraulic conductivity  $k_{eq}$  of PVD-improved ground (Bergado *et al.* 1993b; Bergado and Long 1993)

$$k_{eq} = \frac{\ln(n)}{\ln\left(\frac{n}{q}\right) + \frac{1}{\beta}\ln(q)} k_h \quad (9)$$

Lin and Chang (2009) showed that  $\bar{U}_h$  of PVD-improved ground, derived in terms of the settlement rate, was greater than that derived in terms of the excess pore pressure dissipation rate. The maximum difference in the values of  $\bar{U}_h$ , derived in terms of the settlement and excess pore pressure dissipation rates, was 23% for  $T_h = 1.37$ . The  $s_u$  value of PVD-improved Bangkok clay was estimated to be about twice the value of unimproved clay.

Oliveira *et al.* (2015) compared three types of FE simulations of PVDs installed in Portuguese soft soil: two 2D plane strain simulations and one 3D simulation. The plane strain simulations were performed by: (a) using an equivalent hydraulic conductivity  $k_{eq}$  for PVD-treated soil based on the approach proposed by Asaoka *et al.* (1995), and (b) replacing the axisymmetric flow around the PVDs by flow into equivalent drainage walls (simulated by permeable vertical lines) so that  $k_{h,p} = (2/3)(B/r_{c,eq})^2(1/\mu)k_h$  (Hird *et al.* 1995), where  $B$  is half the spacing of the drainage walls and  $\mu$  is estimated based on Hansbo (1981) but neglecting well resistance. In the 3D simulation, the PVDs were modelled as equivalent square drains using highly permeable FE elements ( $k = 1.16$  cm/s) with sides of  $(b_w+b_p)/2$ . The 2D simulations provided similar results to the computationally intensive 3D simulations with respect to embankment settlement and lateral deformation of subsoil. However, the excess pore pressures were found to be sensitive to the type of analysis performed, because of the distinct flow conditions imposed in each case. The 3D analyses predicted similar excess pore pressures to those obtained from: (a) the 2D analyses performed using Asaoka's  $k_{eq}$ -method, and (b) the field data; however, the 2D simulations with equivalent drainage walls did not predict the excess pore pressures accurately.

Yildiz and Uysal (2015) implemented three different constitutive models, namely, the isotropic Modified Cam-Clay (MCC) and Soft Soil Creep (SSC) models, and the Anisotropic Creep Model with Destructuration (ACM-S), to simulate the time-dependent behaviour of a test embankment constructed on unimproved and PVD-improved soft clay in Haarajoki, Finland. The Haarajoki site consists of structured and sensitive anisotropic soft clay with sensitivity values ranging between 20 and 55. The MCC and SSC models are available by default in PLAXIS, whereas the ACM-S model is a user-defined soil model that accounts for the combined effects of creep, anisotropy and destructuration (the progressive loss or degradation of inter-particle bonding during plastic straining). The SSC model is simply an extension of the SS model described earlier, except that secondary (time-dependent) compression is taken into account. In the 2D FE simulations, the axisymmetric flow of pore water into the PVD was converted into an equivalent plane strain problem via the matching scheme proposed by Hird *et al.* (1995) described earlier, and the matching schemes proposed by Indraratna and Redana (1997) and Chai *et al.* (2001) described in Table 1. The results obtained using the method of Indraratna and Redana (1997) produced the best agreement with the field measurements when compared to those obtained from the other two methods. The SSC and MCC models underestimated the settlement at the center of the embankment by 20% and 28%, respectively, whereas the predictions from the ACM-S model compared reasonably well with the field data.

Chen *et al.* (2016a) performed a 3D FE analysis of a geogrid-reinforced soil (GRS) wall built on unimproved and PVD-improved multilayer soft soil. The GRS wall was constructed at the end of a road embankment in Shanghai, China. On day 118 of the construction (between loading stages), Chen *et al.* (2016a) reported a sudden increase in excess pore water pressure of about 7–10 kPa in some of the pore water pressure meters. The accumulated settlement below the wall and the horizontal movement of the wall toe, up to day 118, were about 400–500 mm and 200 mm, respectively. These observations led to the speculation that the PVDs may have malfunctioned on that day due to bending or kinking caused by large ground deformations. To test this

hypothesis, 3D FE analyses were performed by Chen *et al.* (2016a), wherein the PVDs were modelled using one-dimensional drainage line elements (ignoring well resistance) and were deactivated on day 118 of construction. The FE simulations were performed for three cases: (A)  $r_s/r_{meq} = 1.1$  and  $k_{eq}/k_h = 0.1$ , (B)  $r_s/r_{meq} = 3$  and  $k_{eq}/k_h = 0.3$ , and (C)  $r_s/r_{meq} = 0$  and  $k_{eq}/k_h = 1$  (unimproved case).  $k_{eq}/k_h = 0.1$  provided the best fit between the measured and predicted excess pore pressure profiles, both before and after PVD deactivation. The predicted excess pore pressure profiles, with the PVDs deactivated on day 118, followed the trend of the measured data, thus indicating that the PVDs may have indeed malfunctioned in the field on that day. However, it is unlikely that all the PVDs had failed at the same time in the field, and therefore the results obtained from the simulations performed by deactivating all PVDs on day 118 may not be truly realistic. The factor of safety  $F$  of the embankment was assessed by Chen *et al.* (2016a) using the shear strength reduction (SSR) method as

$$F = \frac{c}{c_r} = \frac{\tan \phi}{\tan \phi_r} \quad (10)$$

where  $c$  and  $c_r$  are the input and reduced values of the cohesive intercept, respectively, and  $\phi$  and  $\phi_r$  are the input and reduced angles of shearing resistance, respectively. The factor of safety of the embankment was 1.19 for the case with PVDs fully functional throughout the analysis, and 1.09 for PVDs deactivated after day 118. These factors of safety were 9% higher than those obtained from 2D FE analyses performed by Xue *et al.* (2014).

Zhou and Chai (2017) investigated the effect of non-uniform consolidation within a PVD unit cell on the average degree of consolidation through laboratory model tests and FE analysis. Non-uniform consolidation implies: (a) spatial variation of the degree of consolidation, i.e., the degree of consolidation at a zone near a drainage boundary would be higher than that of other zones prior to the end of primary consolidation, and (b) non-uniform or layered domains with different hydraulic and compressibility parameters for each layer. The overall smear effect  $k_s/k_h$  was expressed as a product of the mechanical smear effect  $(k_s/k_h)_m$ , which is related to the soil disturbance caused by PVD installation, and the equivalent smear effect  $(k_s/k_h)_e$ , which takes into account the effect of non-uniform consolidation. The concept was applied to two case histories, from which the back-calculated field values of  $k_s/k_h$  were found to be 0.07 and 0.1. These values are much lower than the laboratory-measured  $k_s/k_h$  values reported in Table 3. On the other hand, the estimated values of  $(k_s/k_h)_e$  for  $\bar{U}_h \leq 50\%$  were equal to 0.56 and 0.43. Therefore, by definition, the values of  $(k_s/k_h)_m$  are equal to 0.13 and 0.23, which are now closer to the lower bound of the values reported by Madhav *et al.* (1993) in Table 3. Thus, the non-uniform consolidation-induced equivalent smear parameter  $(k_s/k_h)_e$  proposed by Zhou and Chai (2017) appears to compensate for the difference between the values of  $k_s/k_h$  measured in the laboratory and in the field.

## 5. FIELD STUDIES AND PRACTICAL CONSIDERATIONS

Table 5 summarises the results of 10 field studies performed on PVD-improved soft ground from various parts of the world. The table displays information about the location of the field test, properties of the soft soil layer, PVD details, preload details, and important observations, such as the maximum settlement  $w_{max}$  of the ground surface below the centre of the preload at the end of the monitoring period, the maximum lateral displacement  $\delta_{max}$  of soft ground, the maximum excess pore pressure  $\bar{u}_{max}$  generated, and the increase in undrained shear strength  $\Delta s_u$  and cone resistance  $\Delta q_c$  of soft ground due to its improvement by PVDs. The data presented in Table 5 can be used to validate predictions from analytical and numerical models.

The type of mandrel plays an important role in minimising soil disturbance caused by the installation of PVDs in the field. According to Bo *et al.* (2003), among the four types of mandrels: rhombic, rectangular, square and circular, a rhombic mandrel causes the least disturbance. Further, PVD rigs that push the drain statically into the ground cause less disturbance than rigs that use vibration, and soft clays are prone to greater disturbance than stiff clays (Chu *et al.* 2004). Apart from these practical considerations, Chu *et al.* (2004) discuss additional factors that control the selection of PVDs, quality control tests for PVDs, and selection of PVD design parameters. Among them, the discharge capacity of the PVD, and the apparent opening size (AOS) and cross-plane hydraulic conductivity of the geotextile filter sleeve, are important parameters.

### 5.1 Considerations for PVD Discharge Capacity

Discharge capacity  $q_w$  is an important parameter for the PVD to function well, and is defined as the rate of flow of water per unit hydraulic gradient (Bo 2004). The discharge capacity of PVDs in the field is lower than that specified by manufacturers (Miura and Chai 2000; Chai *et al.* 2004), and can vary from 10 to 2,000 m<sup>3</sup>/year depending on time and magnitude of the confining stress (Bergado *et al.* 1996b; Miura and Chai 2000; Deng *et al.* 2014). For satisfactory performance of PVDs, Holtz *et al.* (1991a) recommend  $q_w$  values to be between 100 and 300 m<sup>3</sup>/year under confining stresses of 300 to 500 kPa. If the operational discharge capacity of the PVD is greater than 100 to 150 m<sup>3</sup>/year under the confining stresses acting on the PVD, then well resistance has negligible effect on the consolidation rate (Holtz 1987; Holtz *et al.* 1991b).

The discharge capacity of the PVD decreases in the field with time due to: (a) squeezing of the filter into the PVD core due to increased surcharge-induced lateral stress from the surrounding soil (Bergado *et al.* 1996b; Tran-Nguyen *et al.* 2010), (b) clogging of the filter openings and drainage channels by clay particles (Miura *et al.* 1998; Chai and Miura 1999), (c) deformation of the PVDs by folding, bending, buckling, or kinking due to large consolidation settlements (Chu *et al.* 2006; Tran-Nguyen *et al.* 2010), (d) changes in hydraulic gradients (Holtz *et al.* 1991a,b; Bergado *et al.* 1996b; Chai *et al.* 2004), and (e) creep of the drain filter (Chai and Miura 1999; Miura and Chai 2000). Furthermore, a vertical compressive strain in excess of 20% can significantly affect the discharge capacity of PVDs (Tran-Nguyen *et al.* 2010).

Chai and Miura (1999) showed that the long-term discharge capacity of PVDs confined in clay is about 5–10% of the short-term discharge capacity of PVDs confined in a rubber membrane. Miura and Chai (2000) recommend that a PVD with at least 3 mm<sup>2</sup> drainage area per channel and a drainage channel shape factor greater than 0.4 mm should be selected for proper drainage functioning of the PVD. The drainage channel shape factor is defined as the ratio of the cross-sectional area of the channel to its perimeter. Bo *et al.* (2016) presented a comprehensive review of the factors that affect the measured discharge capacity of PVDs in the laboratory and concluded that the deformation of PVDs under a folded condition was the most critical factor causing discharge capacity reduction. Table 6 summarises the equations proposed by various researchers for estimation of the required discharge capacity of PVDs to be used in design.

### 5.2 Considerations for Geotextile Filter Sleeve

Two key parameters that indicate the quality of the geotextile filter sleeve are the AOS and the cross-plane hydraulic conductivity of the geotextile filter (Chu *et al.* 2004). The AOS of the geotextile should be small enough to prevent fine soil particles, especially clay particles, from entering the drain, while allowing free and unimpeded flow of pore water. The geotextiles typically used for PVD filter sleeves are non-woven geotextiles with non-uniform pore sizes (Bergado *et al.* 1996a).

Table 5 Field Studies on PVD-Improved Soft Soils from Around the World

Reference	Location	Properties of soft soil layer	PVD details	Preload details	Observations
Almeida <i>et al.</i> (2000)	Rio de Janeiro, Brazil	Soft grey marine clay $H = 12$ m, $w_L = 100$ –350% $PI = 70$ –150%, $w_c = 100$ –500% $OCR = 1.2$ –2.0, $CR = 0.5$	Mebra drain MD7407 $b_w = 100$ mm $b_t = 3$ mm $s = 1.7$ m (triangular)	Embankment $h_e = 3$ m in 2 stages side slope = 1(V):3(H) $\gamma = 17.4$ kN/m <sup>3</sup> , $RC = 95\%$	$w_{max} = 2.4$ m after 4 years $\Delta s_u = 1.5$ –14 kPa $\bar{u}_{max} = 37.6$ kPa at 0.7 m depth
Shen <i>et al.</i> (2005)	Hangzhou Bay, China	Mucky clay $H = 10$ m, $w_L = 43\%$ , $PI = 17\%$ $w_c = 47\%$ , $C_c = 0.65$ , $s_u = 20$ kPa $k_h = 48 \times 10^{-10}$ m/s, $k_v = 32 \times 10^{-10}$ m/s	NW polyolefin filter $b_w = 100$ mm, $b_t = 6$ mm $s = 1.5$ m (triangular) $q_w = 100$ m <sup>3</sup> /year	Embankment $h_e = 5.9$ m in 2 stages $b_{top} = 26$ m, side slope = 1(V):1.5(H) $\gamma = 20$ kN/m <sup>3</sup>	$w_{max} = 1.95$ m after 2.7 years $\delta_{max} = 0.52$ m at 8 m depth $\bar{u}_{max} = 68.4$ kPa at 10 m depth
Bo <i>et al.</i> (2007)	Changi Airport, Singapore	Singapore marine clay $H = 10$ –30 m, $w_c = 40$ –80% $w_L = 75\%$ , $PI = 40$ –60% $C_c = 0.6$ –1.0, $c_v = 0.5$ –1.5 m <sup>2</sup> /yr	$s = 1.5$ m (square)	Embankment $h_e = 6$ m in 2 stages	$w_{max} = 2.4$ m at 1.8 years, $\Delta s_u = 12$ –26 kPa at 1.7 years after PVD installation $\Delta q_c = 18$ –36 kPa at 1.8 years after PVD installation, $\bar{u}_{max} = 120$ kPa at 10 m depth
Lo <i>et al.</i> (2008)	Sydney, Australia	Soft alluvial clay $H = 16$ m, $w_c \approx w_L = 72$ –99% $PI = 54$ –63%, $s_u = 15$ –25 kPa $C_c = 0.7$ –0.9, $c_v = 0.2$ –0.4 m <sup>2</sup> /yr $c_h = 0.5$ –0.8 m <sup>2</sup> /yr	PVC core and geotextile filter $b_w = 100$ mm, $b_t = 4$ mm $s = 1.5$ m (triangular) $q_w > 347$ m <sup>3</sup> /year for $i = 1$ and $\sigma_c \geq 200$ kPa	Geogrid-reinforced embankment $h_e = 5.5$ m in 3 stages $b_{base} = 60$ m $\gamma = 13.5$ kN/m <sup>3</sup> $T_{ult} = 200$ kN/m	$w_{max} = 1.73$ m after 9.3 years $\delta_{max} = 0.14$ m at 6 m depth $T_{max} = 14.6$ kN/m $\bar{u}_{max} = 55$ kPa at 7.7 m depth
Hayashi <i>et al.</i> (2011)	Hokkaido, Japan	Organic peat and soft clay $H = 6$ m, $w_c = 66$ –679%, $e = 2$ –10 $C_c = 0.28$ –5.6, $LOI = 4.3$ –91%	Plastic PVD $b_w = 94$ mm, $b_t = 4$ mm $s = 0.9$ m	Steel grid-reinforced embankment $h_e = 10.6$ m @ 9 cm/day, $b_{top} = 20.2$ m side slope = 1(V):1(H), $T_{ult} = 168$ kN/m	$w = 0.47$ m after 200 days (no PVD) and 73 days (with PVD), $T_{max} = 125$ kN/m $\Delta s_u = 10$ kPa at 68 days after PVD installation
Palmeira <i>et al.</i> (2013)	Santa Catarina, Brazil	Soft clay $H = 9$ m, $w_L = 67\%$ , $PI = 33\%$ $w_c = 100\%$ , $e = 2.3$ , $s_u = 5$ –40 kPa	NW geotextile filter $b_w = 100$ mm, $b_t = 5$ mm $s = 1.35$ m (square)	Geogrid-reinforced embankment $h_e = 3.6$ m @ 35 cm/day, $b_{top} = 13$ m side slope = 1(V):1.5(H), $\gamma = 21$ kN/m <sup>3</sup> $T_{ult} = 200$ kN/m	$w_{max} = 0.27$ m after 47 days $\bar{u}_{max} = 14.5$ kPa at 8 m depth $\delta_{max} = 32$ mm at 5 m depth
Pitchumani and Madhav (2014)	Chennai, India	Soft silty clay $H = 8$ m, $w_L = 45$ –100%, $PI = 20$ –60%, $e = 1.0$ –2.2, $c_v = 0.2$ –1.4 m <sup>2</sup> /yr $c_h = 1.9$ –6.5 m <sup>2</sup> /yr	$b_w = 100$ mm, $b_t = 4$ mm $s = 1.5$ m (triangular)	Surcharge fill $h_e = 2$ m @ 13 cm/day $\gamma = 17$ kN/m <sup>3</sup>	$w_{max} = 85$ mm after 130 days
Xue <i>et al.</i> (2014)	Shanghai, China	Soft Shanghai clay $H = 31$ m, $w_c = 24$ –41% $PI = 15$ –18%, $e = 0.7$ –1.16	$b_w = 100$ mm, $b_t = 4$ mm $s = 1.5$ m (triangular) $q_w = 100$ m <sup>3</sup> /year	Geogrid-reinforced MSE wall $h_e = 7.6$ m, $b_{top} = 37.2$ m, $\gamma = 19$ kN/m <sup>3</sup> side slope = 1(V):1.5(H), $T_{ult} = 70$ kN/m	$w_{max} = 1.1$ m after 250 days $\bar{u}_{max} = 62$ kPa at 2.6 m depth
Wu <i>et al.</i> (2015)	Zhejiang Province, China	Soft marine clay $H = 20$ m, $w_L = 60\%$ , $PI = 40\%$ $w_c = 40\%$ , $e = 1.5$ –2.0, $s_u = 8$ –17 kPa $k_h = 6.9 \times 10^{-9}$ m/s, $k_v = 3 \times 10^{-9}$ m/s	$b_w = 100$ mm $b_t = 6$ mm $s = 1.3$ m (square) $q_w = 100$ m <sup>3</sup> /year	Embankment $h_e = 8$ m in 8 stages, $b_{base} = 93.2$ m side slope = 1(V):0.4(H)–1(V):3(H) $\gamma = 23.5$ kN/m <sup>3</sup>	$w_{max} = 3.34$ m after 2.2 years $\bar{u}_{max} = 70$ kPa at 12 m depth $\Delta s_u = 12$ –16.5 kPa at 1.8 years after PVD installation
Chen <i>et al.</i> (2016b)	Jiangxi Province, China	Soft alluvial silty clay $H = 15$ m, $w_c \approx w_L = 30$ –45%, $PI = 15$ –20%, $e = 0.8$ –1.2, $C_c = 0.1$ –0.4 $k_h = 2.9 \times 10^{-9}$ m/s, $k_v = 5.2 \times 10^{-10}$ m/s	$b_w = 100$ mm $b_t = 4$ mm $s = 1.5$ m (triangular) $q_w = 80$ m <sup>3</sup> /year	Embankment $h_e = 5.3$ m in 8 stages $b_{top} = 12$ m, $b_{base} = 33.6$ m $\gamma = 20$ kN/m <sup>3</sup>	$w_{max} = 0.44$ m after 3.7 years $\bar{u}_{max} = 35$ kPa at 2.5–5 m depth $\delta_{max} = 70$ mm at 6 m depth

Note: PVC = polyvinyl chloride, and MSE = mechanically stabilized earth

Table 6 Estimation of Required Discharge Capacity of PVD

Reference	Equation	Remarks
Xie (1987)	$q_{w,req} \geq 7.85k_h l_d^2 F$	1. Required PVD discharge capacity $q_{w,req}$ for well resistance to be ignored (based on numerical simulations) 2. $F$ is a factor of safety (equal to 4–6). For very soft soil, $F = 10$ (Chu <i>et al.</i> 2006)
Mesri and Lo (1991)	$q_{w,req} = 5k_h l_d^2$	1. Required PVD discharge capacity to minimize well resistance (based on back-analysis of three embankments on PVD-improved ground)
Kamon <i>et al.</i> (1994)	$q_{w,req} = \frac{0.025\pi c_h l_d F}{4T_h}$	1. Equation is based on the average rate of settlement within 10% of the final (primary) settlement. Final settlement is assumed to be 25% of the depth of the soil layer to be improved 2. $T_h$ = time factor for 10% average degree of radial consolidation 3. $F$ is estimated based on Bergado <i>et al.</i> (1996b)
Bergado <i>et al.</i> (1996b)	$F = F_t F_c F_{fc}$	1. Equation is based on the results obtained from laboratory discharge capacity tests and modified triaxial tests on 10 different types of PVDs 2. $F_t$ = reduction factor due to time = 1.25, $F_c$ = reduction factor due to deformation = 2, $F_{fc}$ = reduction factor due to filtration and clogging = 3.5
Bo (2004)	$q_{w,avg} = \frac{\varepsilon_v \pi r_d^2 H l_d \gamma_w}{P_v t_{100}}$	1. Equation is based on initial hydraulic gradient and average flow rate throughout the preloading period. Actual required discharge capacity $q_{w,req}$ may be one or two orders of magnitude higher than the average discharge capacity $q_{w,avg}$ 2. $t_{100}$ = time required for completion of primary consolidation
Tripathi and Nagesha (2010)	$q_{w,req} = \frac{6\pi c_h l_d \gamma_w w_f F}{p_v [\ln(n) - 0.75]}$	1. Equation is based on discharge and hydraulic gradient in PVD when consolidation just starts (i.e., at $t = 0$ ) 2. $w_f$ = final settlement after completion of primary consolidation 3. $F$ is estimated based on Bergado <i>et al.</i> (1996b)

Several soil–geotextile filter retention criteria have been proposed by researchers in terms of relationships between the representative pore size (AOS or  $O_{95}$  and  $O_{50}$ ) of the geotextile and the particle size ( $D_{50}$  and  $D_{85}$ ) of the soil, where  $O_{95}$  corresponds to the particle size (bead size) in mm for which 5% or less by mass passes through the geotextile when tested in accordance with ASTM D4751 (2016). Commonly used filtration criteria for geotextile filters are those proposed by Carroll (1983):  $O_{95}/D_{85} \leq 2$  to 3 and  $O_{50}/D_{50} \leq 10$  to 12; Bergado *et al.* (1993a):  $O_{95}/D_{85} \leq 2$  to 3 and  $O_{50}/D_{50} \leq 18$  to 24 (for Bangkok clay); and Chu *et al.* (2004):  $O_{95}/D_{85} \leq 4$  to 7.5 (for Singapore marine clay). Additional  $O_{95}/D_{85}$  and  $O_{50}/D_{50}$  relationships have been summarised by Bergado *et al.* (1996a). Also, Chu *et al.* (2004) report that  $O_{95} \leq 0.075$  mm for PVD filter sleeves in general, whereas Bergado *et al.* (1996a) report that  $O_{95} \leq 0.09$  mm for PVDs in Bangkok clay.

The cross-plane hydraulic conductivity  $k_g$  of the geotextile filter sleeve should be at least one order of magnitude higher than  $k_h$  (Bergado *et al.* 1993a; Chu *et al.* 2004). However, based on laboratory filtration test results on geotextiles used as filter sleeves for 10 types of PVDs in Bangkok clay, Bergado *et al.* (1996a) recommend that: (a) a more relaxed criterion of  $k_g/k_h \geq 2$  may be adopted, and (b)  $O_{15}/D_{15} \geq 1.5$  to prevent clogging. According to Chu *et al.* (2004), most PVDs have a filter hydraulic conductivity greater than  $10^{-4}$  m/s, which is much higher than the horizontal hydraulic conductivity of soft clay into which PVDs are installed. Indraratna (2017) presented an overview of recent theoretical and practical developments on soft ground improvement using PVDs with surcharge and vacuum preloading.

## 6. CASE HISTORIES

### 6.1 Suvarnabhumi International Airport, Thailand

Moh and Lin (2003) presented a case history of ground improvement using preloading with PVDs for the construction of the Suvarnabhumi International Airport (SIA) at Nong Ngu Hao, Thailand. Extensive soil investigation, comprising of 144 boreholes, 236 field vane shear tests and 97 cone penetration tests, was carried out at the site. The subsoil profile consists of a top 1.5-m-thick weathered crust followed by 6.5 m of very soft-to-soft clay (Bangkok clay), 5.0 m of medium stiff clay and 9.0 m of stiff clay (Figure 11). A dense sand layer exists below the stiff clay at a depth of 25 m. The very soft-to-soft clay layer has a maximum water

content of 112% (close to the liquid limit) at a depth of 6.5 m. The undrained field vane shear strength increases from 15 kPa at a depth of 1.5 m to 85 kPa at a depth of 15 m below the ground surface.

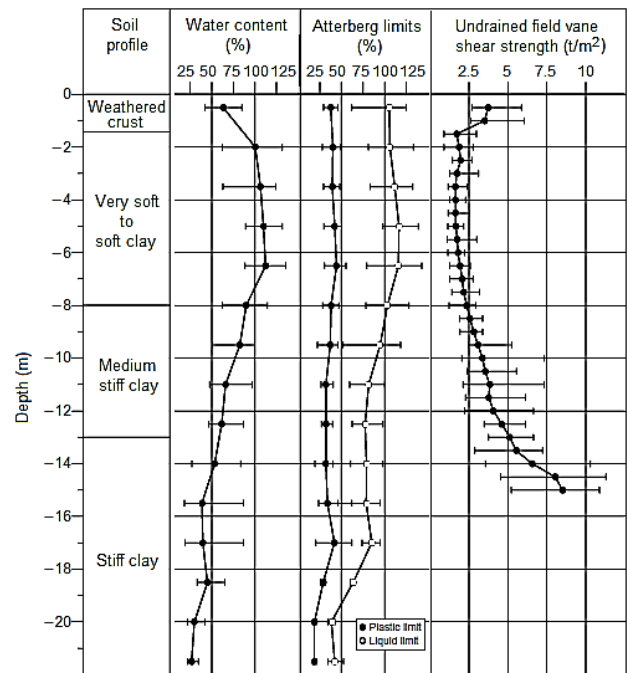


Figure 11 Water content, Atterberg limits and undrained shear strength profiles at SIA site (modified from Moh and Lin 2003)

10-m-long PVDs were installed at 1 m spacing in a square pattern. The PVDs were connected to a 150-cm-thick sand blanket over which a 3.8-m-high embankment was constructed in two stages using crushed rock. The embankment was supported by 15-m-wide and 1.7-m-high berms with 1(V):4(H) side slope. The waiting period between each preload stage was three months and the preload removal criteria were as follows: (a) minimum waiting period of 6 or 11 months, (b) minimum 80% primary consolidation of soft ground, and (c) maximum settlement ratio of 2–4% (i.e., the ratio of the previous month’s settlement to the accumulated settlement).

The maximum surface settlement of the embankment, attained after 750 days of monitoring, was equal to 440 mm for unimproved Bangkok clay and 1,349 mm for PVD-improved Bangkok clay (Figure 12). Furthermore, the time taken to reach a settlement of 440 mm was 750 days for unimproved Bangkok clay, but just 460 days for PVD-improved Bangkok clay; a time saving of 38.7%. Thus, the PVDs were instrumental in accelerating the consolidation of soft Bangkok clay. Maximum lateral deformation was equal to 190 mm at a depth of 4 m below the ground surface. Changes in water content and undrained shear strength of Bangkok clay were assessed before and after ground improvement with PVDs. The water content reduced by 20–25%, whereas the undrained shear strength increased by 100%, due to the use of preloading with PVDs. Consequently, the response of the upper stratum of very soft to soft clay improved to that of medium stiff clay based on the soil properties reported by Moh and Lin (2003).

**6.2 Hangzhou–Ningbo Expressway, China**

Shen *et al.* (2005) monitored the behaviour of two embankment sections along the 145-km-long Hangzhou–Ningbo (HN) expressway constructed on unimproved and PVD-improved soft ground. The subsoil profile at the site consists of a top 1.0–1.5-m-thick weathered crust followed by 4 m of silty clay, 10–11 m of very soft mucky clay, 3–4 m of mucky-silty clay, and 3–5 m of medium to stiff silty clay (Figure 13). The solid horizontal lines in Figure 13 correspond to PVD-improved ground and the dashed horizontal lines correspond to unimproved ground because the soil layer thicknesses were different at the two test sections. The soft clay layers have water contents greater than their liquid limits with relatively high compression indices ( $C_c = 0.4–0.6$ ) and low undrained shear strength ( $s_u = 20$  kPa).

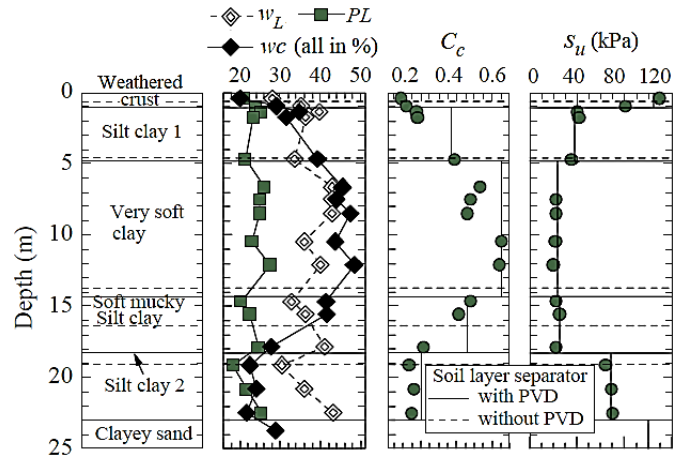


Figure 13 Subsoil profile at HN expressway site (modified from Shen *et al.* 2005)

19-m-long PVDs, with 100 mm × 6 mm cross-section and 1580 m<sup>3</sup>/year discharge capacity (manufacturer’s value), were installed at 1.5 m spacing in a triangular pattern. The PVD core and filter consisted of corrugated polyethylene and non-woven polyolefin materials, respectively. The PVDs were connected to a 50-cm-thick sand mat ( $k > 0.001$  m/s) over which a 5.9-m-high embankment (for PVD-improved ground) and a 4.7-m-high embankment (for unimproved ground) were constructed using decomposed granite ( $\gamma = 20$  kN/m<sup>3</sup>). The top width and side slopes of the embankments were 26 m and 1(V):1.5(H), respectively.

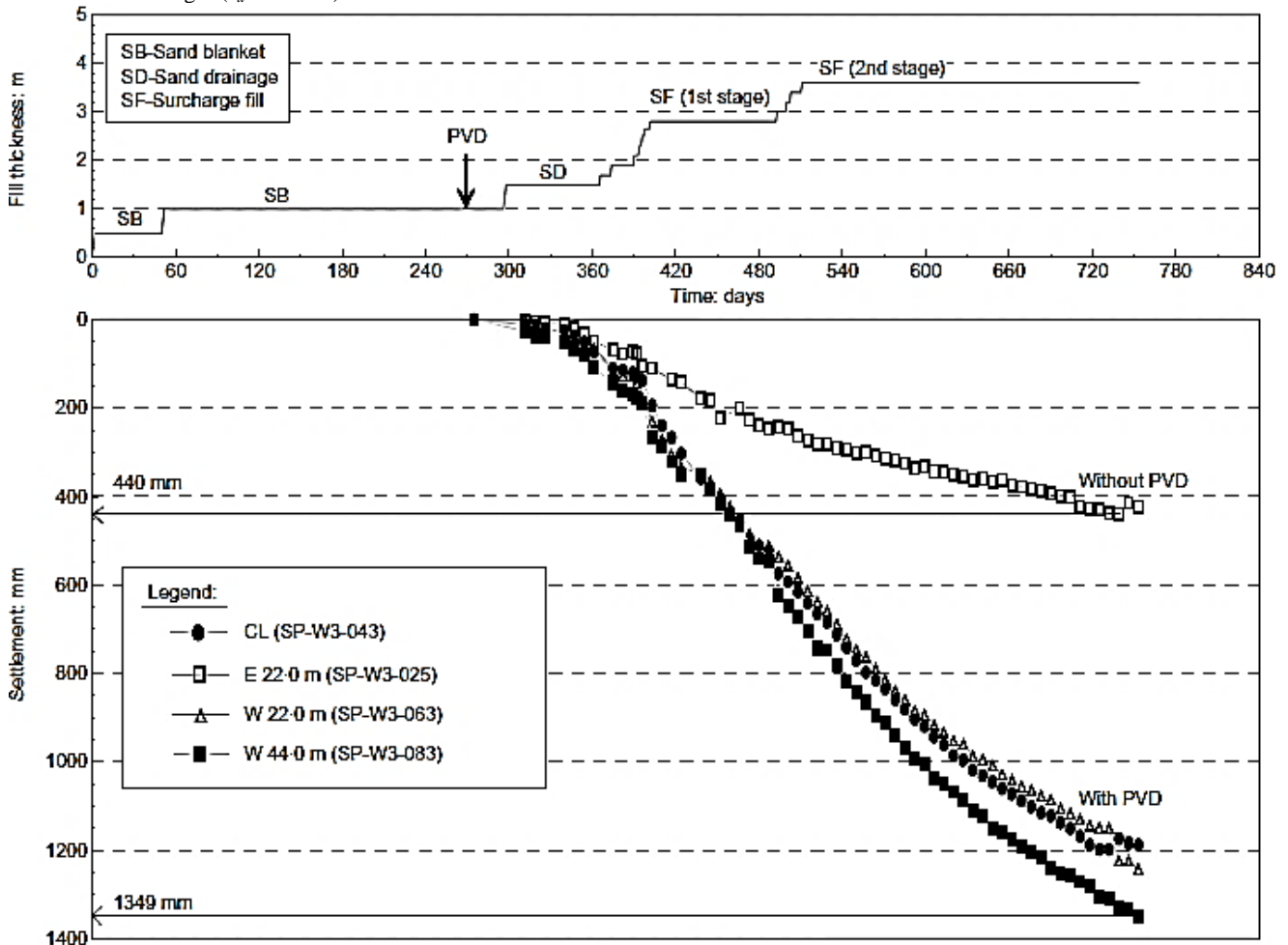
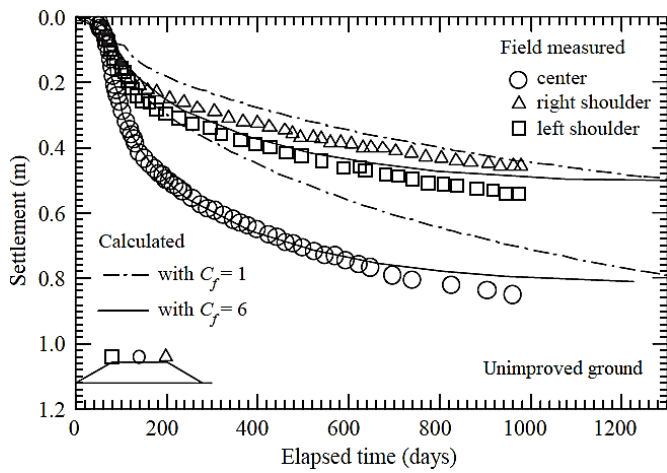
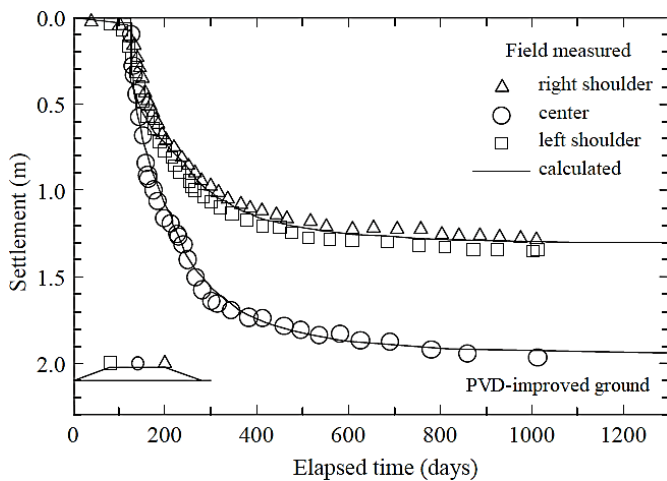


Figure 12 Surface settlement–time profiles of SIA embankment with and without the inclusion of PVDs (Moh and Lin 2003)

The surface settlement–time profiles at the centre, left shoulder, and right shoulder of the embankment on unimproved and PVD-improved ground are shown in Figures 14(a) and (b), respectively. Primary consolidation of PVD-improved ground was achieved in about 600 days, whereas unimproved ground needed a lot more time (close to 1000 days) for completion of primary consolidation. The maximum lateral displacements at the end of embankment construction were 90 mm at 4 m depth (for unimproved ground) and 520 mm at 8 m depth (for PVD-improved ground). By curve-fitting the FE-simulated settlement–time profiles to the measured data, Shen *et al.* (2005) found the operational discharge capacity of the PVD to range between 79 and 100 m<sup>3</sup>/year, which is about 5–6% of the manufacturer-provided value of 1580 m<sup>3</sup>/year. Thus, the discharge capacity of PVDs in the field can be significantly lower than the value provided by the manufacturer, and this aspect should be considered in design.



(a)



(b)

Figure 14 Measured and FE-simulated surface settlement–time profiles of embankment on: (a) unimproved ground and (b) PVD-improved ground (Shen *et al.* 2005)

**7. CONCLUDING REMARKS**

Preloading with PVDs is one of the most effective techniques for stabilization of soft soils. Various developments in PVD research, during the past two to three decades, have been reviewed and organized into sections covering analytical, laboratory, numerical and field studies. Emphasis was given to conventional PVDs without the use of vacuum, thermal and electro-osmosis techniques.

Summary tables, which provide quick and easy access to the latest information from various research efforts, have been prepared for the benefit of academics and practitioners. Significant analytical improvements have been made to the classical radial consolidation theory of Hansbo (1981), such as: (1) separation of the single disturbed zone into an inner smear zone and transition zone, (2) conversion of axisymmetric unit cell parameters into equivalent plane strain parameters, (3) non-linear consolidation via  $e-\log\sigma'_v$  and  $e-\log k_h$  relationships, (4) spatial variations (linear, bilinear and parabolic variations) of the horizontal hydraulic conductivity of soil in the disturbed zone, inner smear zone and transition zone, (5) time-dependent preloading, (6) non-Darcian flow, (7) exponential decay of discharge capacity with time, (8) effective stress–dependent  $c_h$ , and (9) use of non-traditional PVD installation patterns, such as circular drain ring and parallel drain wall patterns.

The radii and horizontal hydraulic conductivities of the inner smear zone and the transition zone, measured from experimental studies by various researchers, have been tabulated. The horizontal hydraulic conductivity of soil in the inner smear zone, immediately adjacent to the PVD, reduces to about 0.2 to 0.35 times the horizontal hydraulic conductivity  $k_h$  of soil in the undisturbed zone, increases gradually with radial distance in the transition zone along a linear or bilinear path, and finally approaches the value of  $k_h$  at the boundary between the transition zone and the undisturbed zone. The radius  $r_{sm}$  of the inner smear zone varies from 1.5 to 3.7 times the equivalent radius  $r_{m,eq}$  of the mandrel, whereas the radius  $r_{tr}$  of the transition zone varies from 5.2 to 10.3 times  $r_{m,eq}$  depending on the type of soil and the size and installation rate of the mandrel.

The field studies highlight the successful implementation of PVDs for ground improvement worldwide. Some practical considerations concerning the discharge capacity of PVDs, and the apparent opening size and cross-plane hydraulic conductivity of the geotextile filter sleeve, have been discussed. Equations proposed by various researchers for estimation of the required discharge capacity of PVDs have been tabulated. Finally, the review is complemented by two case histories of ground improvement using preloading with PVDs, one in Thailand and the other in China. Both case histories clearly highlight the main advantage of PVDs, which is to accelerate the consolidation of soft soils so that construction time can be reduced significantly.

**8. ACKNOWLEDGEMENTS**

The authors thank the Editors, Prof. G. Madhavi Latha and Dr. A. Murali Krishna, for the invitation to contribute to the special issue of the Geotechnical Engineering Journal of the Southeast Asian Geotechnical Society (SEAGS) & Association of Geotechnical Societies in Southeast Asia (AGSSEA) in honour of Prof. Madhav Madhira.

**9. REFERENCES**

Abuel-Naga, H. M., Bergado, D. T., and Gniel, J. (2015) “Design chart for prefabricated vertical drains improved ground”. *Geotextiles and Geomembranes*, 43, pp537–546.

Abuel-Naga, H. M., Pender, M. J., and Bergado, D. T. (2012) “Design curves of prefabricated vertical drains including smear and transition zones effects”. *Geotextiles and Geomembranes*, 32, pp1–9.

Abuel-Naga, H., and Bouazza, A. (2009) “Equivalent diameter of a prefabricated vertical drain”. *Geotextiles and Geomembranes*, 27, Issue 3, pp227–231.

Almeida, M. S. S., Santa Maria, P. E. L., Martins, I. S. M., Spotti, A. P., and Coelho, L. B. M. (2000) “Consolidation of a very soft clay with vertical drains”. *Geotechnique*, 50, Issue 6, pp633–643.

Arulrajah, A., Nikraz, H., and Bo, M. W. (2005) “Finite element modelling of marine clay deformation under reclamation fills”. *Ground Improvement*, 9, Issue 3, pp105–118.

- Asaoka, A., Nakano, M., Fernando, G. S. K., and Nozu, M. (1995) "Mass permeability concept in the analysis of treated ground with sand drains". *Soils and Foundations*, 35, Issue 3, pp43–53.
- Asha, B. S., and Mandal, J. N. (2015) "Laboratory performance tests on natural prefabricated vertical drains in marine clay". *Proceedings of the ICE – Ground Improvement*, 168, Issue 1, pp45–65.
- ASTM D4751 (2016). *Standard Test Methods for Determining Apparent Opening Size of a Geotextile*. ASTM International, West Conshohocken, PA, USA.
- Basu, D., Basu, P., and Prezzi, M. (2013) "A rational approach to the design of vertical drains considering soil disturbance". *Proceedings of Geo-Congress 2013*, San Diego, CA, pp551–566.
- Basu, D., Prezzi, M., and Madhav, M. R. (2010b) "Effect of soil disturbance on consolidation by prefabricated vertical drains installed in a rectangular pattern". *Geotechnical and Geological Engineering*, 28, pp61–77.
- Basu, D., Prezzi, M., and Basu, P. (2010a) "Analysis of PVD-enhanced consolidation with soil disturbance". *Proceedings of the ICE – Ground Improvement*, 163, Issue 4, pp237–249.
- Basu, D., and Prezzi, M. (2010) "Design charts for vertical drains considering soil disturbance". *Proceedings of GeoFlorida 2010: Advances in Analysis, Modeling and Design*, Orlando, FL, USA, pp420–429.
- Basu, D., and Prezzi, M. (2009) "Design of prefabricated vertical drains considering soil disturbance". *Geosynthetics International*, 16, Issue 3, pp147–157.
- Basu, D., and Prezzi, M. (2008) "Effect of soil disturbance on consolidation aided by prefabricated vertical drains installed in a triangular pattern". *Proceedings of GeoCongress 2008*, New Orleans, LA, DOI: 10.1061/40972(311)89, pp718–725.
- Basu, D., and Prezzi, M. (2007) "Effect of the smear and transition zones around prefabricated vertical drains installed in a triangular pattern on the rate of soil consolidation". *International Journal of Geomechanics*, 7, Issue 1, pp34–43.
- Basu, D., Basu, P., and Prezzi, M. (2006) "Analytical solutions for consolidation aided by vertical drains". *Geomechanics and Geoengineering*, 1, Issue 1, pp63–71.
- Basu, D., and Madhav, M. R. (2000) "Effect of prefabricated vertical drain clogging on the rate of consolidation: a numerical study". *Geosynthetics International*, 7, Issue 3, pp189–215.
- Bellezza, I., and Fentini, R. (2008) "Prefabricated vertical drains: a simplified design procedure". *Proceedings of the ICE – Ground Improvement*, 161, Issue 4, pp173–178.
- Bergado, D. T., Manivannan, T., and Balasubramaniam, A. S. (1996b) "Proposed criteria for discharge capacity of prefabricated vertical drains". *Geotextiles and Geomembranes*, 14, Issue 9, pp481–505.
- Bergado, D. T., Manivannan, R., and Balasubramaniam, A. S. (1996a) "Filtration criteria for prefabricated vertical drain geotextile filter jackets in soft Bangkok clay". *Geosynthetics International*, 3, Issue 1, pp63–83.
- Bergado, D. T., Mukherjee, K., Alfaro, M. C., and Balasubramaniam, A. S. (1993b) "Prediction of vertical-band-drain performance by finite-element method". *Geotextiles and Geomembranes*, 12, Issue 6, pp567–586.
- Bergado, D. T., Alfaro, M. C., and Balasubramaniam, A. S. (1993a) "Improvement of soft Bangkok clay using vertical drains". *Geotextiles and Geomembranes*, 12, Issue 7, pp615–663.
- Bergado, D. T., and Long, P. V. (1993) "Numerical analysis of embankment on subsiding ground improved by vertical drains". *Geotechnical Engineering Bulletin*, 2, Issue 3, pp177–188.
- Bergado, D. T., Asakami, H., Alfaro, M. C., and Balasubramaniam, A. S. (1991) "Smear effects on vertical drains on soft Bangkok clay". *Journal of Geotechnical Engineering, ASCE*, 117, Issue 10, pp1509–1530.
- Bo, M. W. (2004) "Discharge capacity of prefabricated vertical drain and their field measurements". *Geotextiles and Geomembranes*, 22, Issues 1–2, pp37–48.
- Bo, M. W., Arulrajah, A., Horpibulsuk, S., Chinkulkijniwat, A., and Leong, M. (2016) "Laboratory measurements of factors affecting discharge capacity of prefabricated vertical drain materials". *Soils and Foundations*, 56, Issue 1, pp129–137.
- Bo, M. W., Arulrajah, A., and Nikraz, H. (2007) "Preloading and prefabricated vertical drains design for foreshore land reclamation projects: a case study". *Ground Improvement*, 11, Issue 2, pp67–76.
- Bo, M. W., Chu, J., Low, B. K., and Choa, V. (2003) *Soil Improvement: Prefabricated Vertical Drain Technique*. ISBN 981-243-044-X, Thomson Learning, Singapore, p341.
- Carroll, R. G. (1983) "Geotextile filter criteria". *Transportation Research Record: Journal of the Transportation Research Board*, Issue 916, pp46–53.
- Chai, J.-C., and Xu, F. (2015) "Experimental investigation of lateral displacement of PVD-improved deposit". *Geomechanics and Engineering*, 9, Issue 5, pp585–599.
- Chai, J.-C., Miura, N., and Nomura, T. (2004) "Effect of hydraulic radius on long-term drainage capacity of geosynthetic drains". *Geotextiles and Geomembranes*, 22, Issues 1–2, pp3–16.
- Chai, J.-C., Shen, S.-L., Miura, N., and Bergado, D. T. (2001) "Simple method of modeling PVD-improved subsoil". *Journal of Geotechnical and Geoenvironmental Engineering*, 127, Issue 11, pp965–972.
- Chai, J.-C., and Miura, N. (1999) "Investigation of factors affecting vertical drain behavior". *Journal of Geotechnical and Geoenvironmental Engineering*, 125, Issue 3, pp216–226.
- Chen, J., Shen, S.-L., Yin, Z.-Y., Xu, Y.-S., and Horpibulsuk, S. (2016b) "Evaluation of effective depth of PVD improvement in soft clay deposit: A field case study". *Marine Georesources and Geotechnology*, 34, Issue 5, pp420–430.
- Chen, J.-F., Tolooiyan, A., Xue, J.-F., and Shi, Z.-M. (2016a) "Performance of a geogrid reinforced soil wall on PVD drained multilayer soft soils". *Geotextiles and Geomembranes*, 44, Issue 3, pp219–229.
- Chu, J., Bo, M. W., and Choa, V. (2006) "Improvement of ultra-soft soil using prefabricated vertical drains". *Geotextiles and Geomembranes*, 24, Issue 6, pp339–348.
- Chu, J., Bo, M. W., and Choa, V. (2004) "Practical considerations for using vertical drains in soil improvement projects". *Geotextiles and Geomembranes*, 22, Issues 1–2, pp101–117.
- Dastidar, A. G., Gupta, S., and Ghosh, T. K. (1969) "Application of sand-wick in a housing project". *Proceedings of 7<sup>th</sup> International Conference on Soil Mechanics and Foundation Engineering*, Mexico, pp59–64.
- Davis, E. H., and Raymond, G. P. (1965) "A non-linear theory of consolidation". *Geotechnique*, 15, Issue 2, pp161–173.
- Deng, Y.-B., Liu, G.-B., Indraratna, B., Rujikiatkamjorn, C., and Xie, K.-H. (2017) "Model test and theoretical analysis for soft soil foundations improved by prefabricated vertical drains". *International Journal of Geomechanics*, 17, Issue 1, DOI:10.1061/(ASCE)GM.1943-5622.0000711.
- Deng, Y.-B., Liu, G.-B., Lu, M.-M., and Xie, K.-H. (2014) "Consolidation behavior of soft deposits considering the variation of prefabricated vertical drain discharge capacity". *Computers and Geotechnics*, 62, pp310–316.
- Deng, Y.-B., Xie, K.-H., Lu, M.-M., Tao, H.-B., and Liu, G.-B. (2013) "Consolidation by prefabricated vertical drains considering the time dependent well resistance". *Geotextiles and Geomembranes*, 36, pp20–26.
- Fang, Z., and Yin, J.-H. (2006) "Physical modelling of consolidation of Hong Kong marine clay with prefabricated vertical drains". *Canadian Geotechnical Journal*, 43, Issue 6, pp638–652.
- Ghandeharioon, A., Indraratna, B., and Rujikiatkamjorn, C. (2012) "Laboratory and finite-element investigation of soil disturbance

- associated with the installation of mandrel-driven prefabricated vertical drains". *Journal of Geotechnical and Geoenvironmental Engineering*, 138, Issue 3, pp295–308.
- Ghandeharioon, A., Indraratna, B., and Rujikiatkamjorn, C. (2010) "Analysis of soil disturbance associated with mandrel-driven prefabricated vertical drains using an elliptical cavity expansion theory". *International Journal of Geomechanics*, 10, Issue 2, pp53–64.
- Hansbo, S. (1986) "Preconsolidation of soft compressible subsoil by the use of prefabricated vertical drains". *Annales des travaux publics de Belgique*, 6, pp553–563.
- Hansbo, S. (1981) "Consolidation of fine-grained soils by prefabricated drains", *Proceedings of 10<sup>th</sup> International Conference on Soil Mechanics and Foundation Engineering*, Stockholm, 3, pp677–682.
- Hansbo, S. (1979) "Consolidation of clay by band-shaped prefabricated drains". *Ground Engineering*, 12, Issue 5, pp16–25.
- Hansbo, S. (1960) "Consolidation of clay with special reference to influence of vertical drain", *Proceedings of the Royal Swedish Geotechnical Institute*, No. 18, p160.
- Hayashi, H., Nishimoto, S., and Takahashi, M. (2011) "Field performance of PVD combined with reinforced embankment on peaty ground". *Soils and Foundations*, 51, Issue 1, pp191–201.
- Hird, C. C., and Moseley, V. J. (2000) "Model study of seepage in smear zones around vertical drains in layered soil". *Geotechnique*, 50, Issue 1, pp89–97.
- Hird, C. C., Pyrah, I. C., Russell, D., and Cinicioglu, F. (1995) "Modelling the effect of vertical drains in two-dimensional finite element analyses of embankments on soft ground". *Canadian Geotechnical Journal*, 32, Issue 5, pp795–807.
- Holtz, R. D., Lancellotta, R., Jamiolkowski, M., and Pedroni, S. (1991b) "Laboratory testing of prefabricated "wick" drains", *Proceedings of International Conference on Geotechnical Engineering for Coastal Development*, Yokohama, pp311–316.
- Holtz, R. D., Jamiolkowski, M., Lancellotta, R., and Pedroni, R. (1991a) *Prefabricated Vertical Drains: Design and Performance*, Butterworth-Heinemann, Oxford, UK.
- Holtz, R. D. (1987) "Preloading with prefabricated vertical strip drains". *Geotextiles and Geomembranes*, 6, Issues 1–3, pp109–131.
- Howell, R., Rathje, E. M., Kamai, R., and Boulanger, R. (2012) "Centrifuge modeling of prefabricated vertical drains for liquefaction remediation". *Journal of Geotechnical and Geoenvironmental Engineering*, 138, Issue 3, pp262–271.
- Howell, R., Kamai, R., Conlee, C., Rathje, E. M., Boulanger, R., Marinucci, A., and Rix, G. (2009) *Evaluation of the Effectiveness of Prefabricated Vertical Drains for Liquefaction Remediation: Centrifuge Data Report for RLH01*, Data Rep. UCD/CGMDR-0801, Center for Geotechnical Modeling, University of California, Davis, CA.
- Huang, C., Deng, Y., and Chen, F. (2016) "Consolidation theory for prefabricated vertical drains with elliptic cylindrical assumption". *Computers and Geotechnics*, 77, pp156–166.
- Indraratna, B. (2017) "Recent advances in vertical drains and vacuum preloading for soft ground stabilization", 4<sup>th</sup> Louis Menard Lecture, *Proceedings of 19<sup>th</sup> International Conference on Soil Mechanics and Geotechnical Engineering*, Seoul, pp145–170.
- Indraratna, B., Nguyen, T. T., Carter, J., and Rujikiatkamjorn, C. (2016) "Influence of biodegradable natural fibre drains on the radial consolidation of soft soil". *Computers and Geotechnics*, 78, pp171–180.
- Indraratna, B., Perera, D., Rujikiatkamjorn, C., and Kelly, R. (2015) "Soil disturbance analysis due to vertical drain installation". *Proceedings of the ICE – Geotechnical Engineering*, 168, Issue 3, pp236–246.
- Indraratna, B., Attya, A., and Rujikiatkamjorn, C. (2009) "Experimental investigation on effectiveness of a vertical drain under cyclic loads". *Journal of Geotechnical and Geoenvironmental Engineering*, 135, Issue 6, pp835–839.
- Indraratna, B., Aljorany, A., and Rujikiatkamjorn, C. (2008) "Analytical and numerical modeling of consolidation by vertical drain beneath a circular embankment". *International Journal of Geomechanics*, 8, Issue 3, pp199–206.
- Indraratna, B., Rujikiatkamjorn, C., and Sathananthan, I. (2005) "Radial consolidation of clay using compressibility indices and varying horizontal permeability". *Canadian Geotechnical Journal*, 42, Issue 5, pp1330–1341.
- Indraratna, B., and Redana, I. W. (2000) "Numerical modeling of vertical drains with smear and well resistance installed in soft clay". *Canadian Geotechnical Journal*, 37, Issue 1, pp132–145.
- Indraratna, B., and Redana, I. W. (1998b) "Development of the smear zone around vertical band drains". *Proceedings of the ICE – Ground Improvement*, 2, Issue 4, pp165–178.
- Indraratna, B., and Redana, I. W. (1998a) "Laboratory determination of smear zone due to vertical drain installation". *Journal of Geotechnical and Geoenvironmental Engineering*, 124, Issue 2, pp180–184.
- Indraratna, B., and Redana, I. W. (1997) "Plane strain modeling of smear effects associated with vertical drains". *Journal of Geotechnical Engineering*, ASCE, 123, Issue 5, pp474–478.
- Kamon, M., Pradhan, T. B. S., Suwa, S., Hanyo, T., Akai, T., and Imanishi, H. (1994) "The evaluation of discharge capacity of prefabricated band shaped drains", *Proceedings of Symposium on Geotextile Test Methods, JSSMFE*, Tokyo, pp77–82.
- Khan, P. A., Madhav, M. R., and Reddy, E. S. (2010) "Consolidation of thick clay layer by radial flow – non-linear theory". *Geomechanics and Engineering*, 2, Issue 2, pp157–160.
- Kjellman, W. (1948) "Accelerating consolidation of fine-grained soils by means of cardboard wicks", *Proceedings of 2<sup>nd</sup> International Conference on Soil Mechanics and Foundation Engineering*, London, pp302–305.
- Lam, L. G., Bergado, D. T., and Hino, T. (2015) "PVD improvement of soft Bangkok clay with and without vacuum preloading using analytical and numerical analyses". *Geotextiles and Geomembranes*, 43, Issue 6, pp547–557.
- Lei, G. H., Zheng, Q., Ng, C. W. W., Chiu, A. C. F., and Xu, B. (2015) "An analytical solution for consolidation with vertical drains under multi-ramp loading". *Geotechnique*, 65, Issue 7, pp531–547.
- Lin, D. G., and Chang, K. T. (2009) "Three-dimensional numerical modelling of soft ground improved by prefabricated vertical drains". *Geosynthetics International*, 16, Issue 5, pp339–353.
- Liu, K.-W., and Rowe, R. K. (2015) "Numerical modelling of prefabricated vertical drains and surcharge on reinforced floating column-supported embankment behaviour". *Geotextiles and Geomembranes*, 43, Issue 6, pp493–505.
- Lo, S. R., Mak, J., Gnanendran, C. T., Zhang, R., and Manivannan, G. (2008) "Long-term performance of a wide embankment on soft clay improved with prefabricated vertical drains". *Canadian Geotechnical Journal*, 45, Issue 8, pp1073–1091.
- Lu, M., Sloan, S. W., Indraratna, B., Jing, H., and Xie, K. (2016) "A new analytical model for consolidation with multiple vertical drains". *International Journal for Numerical and Analytical Methods in Geomechanics*, 40, Issue 11, pp1623–1640.
- Lu, M., Wang, S., Sloan, S. W., Indraratna, B., and Xie, K. (2015) "Nonlinear radial consolidation of vertical drains under a general time-variable loading". *International Journal for Numerical and Analytical Methods in Geomechanics*, 39, Issue 1, pp51–62.
- Madhav, M. R., Park, Y.-M., and Miura, N. (1993) "Modelling and study of smear zones around band shaped drains". *Soils and Foundations*, 33, Issue 4, pp135–147.

- Mesri, G., and Lo, D. O. K. (1991) "Field performance of prefabricated vertical drains", Proceedings of International Conference on Geotechnical Engineering for Coastal Development, Yokohama, pp231–236.
- Miura, N., and Chai, J.-C. (2000) "Discharge capacity of prefabricated vertical drains confined in clay". Geosynthetics International, 7, Issue 2, pp119–135.
- Miura, N., Chai, J.-C., and Toyota, K. (1998) "Investigation on some factors affecting discharge capacity of prefabricated vertical drain", Proceedings of 6<sup>th</sup> International Conference on Geosynthetics, Atlanta, GA, 2, pp845–850.
- Moh, Z. C., and Lin, P. C. (2003) "From cobra swamp to international airport: ground improvement at Suvarnabhumi International Airport, Thailand". Proceedings of the ICE – Ground Improvement, 7, Issue 2, pp87–102.
- Oliveira, P. J. V., Cruz, R. F. P. M. L., Lemos, L. J. L., and Sousa, J. N. V. A. (2015) "Numeric modelling of vertical drains: two- and three-dimensional analyses". Proceedings of the ICE – Ground Improvement, 168, Issue 2, pp144–156.
- Onoue, A., Ting, N. H., Germaine, J. T., and Whitman, R. V. (1991) "Permeability of disturbed zone around vertical drains", Proceedings of ASCE Geotechnical Engineering Congress, Reston, VA, pp879–890.
- Palmeira, E. M., Fabel, A. R. S., and Araujo, G. L. S. (2013) "Behaviour of geogrid reinforced abutments on soft soil". Geotechnical Engineering, Journal of the SEAGS & AGSSEA, 44, Issue 4, pp9–16.
- Pitchumani, N. K., and Madhav, M. R. (2014). "A field monitoring study on pre-compression of soft deposit for ballastless railway tracks for Chennai metro rail: Evaluation of compressibility parameters". Indian Geotechnical Journal, 44, Issue 4, pp449–457.
- Rixner, J. J., Kraemer, S. R., and Smith, A. D. (1986) Prefabricated Vertical Drains. Engineering Guidelines, FWH/RD-86/168, Vol. I, Federal Highway Administration, McLean, VA, p117.
- Roscoe, K. H., and Burland, J. B. (1968) On the Generalized Stress-Strain Behaviour of Wet Clay, Engineering Plasticity, Cambridge University Press, Cambridge, UK, pp535–609.
- Rujikiatkamjorn, C., and Indraratna, B. (2015) "Effect of drain installation patterns on rate of consolidation". Proceedings of the ICE – Ground Improvement, 168, Issue 4, pp236–245.
- Rujikiatkamjorn, C., Ardana, M. D. W., Indraratna, B., and Leroueil, S. (2013) "Conceptual model describing smear zone caused by mandrel action". Geotechnique, 63, Issue 16, pp1377–1388.
- Rujikiatkamjorn, C., and Indraratna, B. (2010) "Radial consolidation modelling incorporating the effect of a smear zone for a multilayer soil with downdrag caused by mandrel". Canadian Geotechnical Journal, 47, Issue 9, pp1024–1035.
- Saowapakpiboon, J., Bergado, D. T., Youwai, S., Chai, J.-C., Wanthong, P., and Vootipruex, P. (2010) "Measured and predicted performance of prefabricated vertical drains (PVDs) with and without vacuum preloading". Geotextiles and Geomembranes, 28, Issue 1, pp1–11.
- Sathananthan, I., Indraratna, B., and Rujikiatkamjorn, C. (2008) "Evaluation of smear zone extent surrounding mandrel driven vertical drains using the cavity expansion theory". International Journal of Geomechanics, 8, Issue 6, pp355–365.
- Sathananthan, I., and Indraratna, B. (2006b) "Laboratory evaluation of smear zone and correlation between permeability and moisture content". Journal of Geotechnical and Geoenvironmental Engineering, 132, Issue 7, pp942–945.
- Sathananthan, I., and Indraratna, B. (2006a) "Plane-strain lateral consolidation with non-Darcian flow". Canadian Geotechnical Journal, 43, Issue 2, pp119–133.
- Sengul, T., Edil, T., and Ozaydin, K. (2016) "Laboratory determination of smear and transition zones due to prefabricated vertical drain installation". Marine Georesources & Geotechnology, DOI:10.1080/1064119X.2016.1256924.
- Sharma, J. S., and Xiao, D. (2000) "Characterization of a smear zone around vertical drains by large-scale laboratory tests". Canadian Geotechnical Journal, 37, Issue 6, pp1265–1271.
- Shen, S.-L., Chai, J.-C., Hong, Z.-S., and Cai, F.-X. (2005) "Analysis of field performance of embankments on soft clay deposit with and without PVD-improvement". Geotextiles and Geomembranes, 23, Issue 6, pp463–485.
- Shin, D.-H., Lee, C., Lee, J.-S., and Lee, W. (2009) "Detection of smear zone using micro-cone and electrical resistance probe". Canadian Geotechnical Journal, 46, Issue 6, pp719–726.
- Tarefder, R. A., Zaman, M. M., Lin, D. G., and Bergado, D. T. (2009) "Finite element modeling of soft ground with PVD under vacuum and embankment preloading". International Journal of Geotechnical Engineering, 3, Issue 2, pp233–249.
- Tran-Nguyen, H. H., Edil, T. B., and Schneider, J. A. (2010) "Effect of deformation of prefabricated vertical drains on discharge capacity". Geosynthetics International, 17, Issue 6, pp431–442.
- Tripathi, K. K., and Nagesha, M. S. (2010) "Discharge capacity requirement of prefabricated vertical drains". Geotextiles and Geomembranes, 28, Issue 1, pp128–132.
- Walker, R., Indraratna, B., and Rujikiatkamjorn, C. (2012) "Vertical drain consolidation with non-Darcian flow and void-ratio-dependent compressibility and permeability". Geotechnique, 62, Issue 11, pp985–997.
- Walker, R., and Indraratna, B. (2007) "Vertical drain consolidation with overlapping smear zones". Geotechnique, 57, Issue 5, pp463–467.
- Walker, R., and Indraratna, B. (2006) "Vertical drain consolidation with parabolic distribution of permeability in smear zone". Journal of Geotechnical and Geoenvironmental Engineering, 132, Issue 7, pp937–941.
- Wu, H.-N., Shen, S.-L., Ma, L., Yin, Z.-Y., and Horpibulsuk, S. (2015) "Evaluation of the strength increase of marine clay under staged embankment loading: A case study". Marine Georesources & Geotechnology, 33, Issue 6, pp532–541.
- Xie, K.-H. (1987) Consolidation Theories and Optimisation Design for Vertical Drains, Ph.D. Thesis, Zhejiang University, China.
- Xue, J.-F., Chen, J.-F., Liu, J.-X., and Shi, Z.-M. (2014) "Instability of a geogrid reinforced soil wall on thick soft Shanghai clay with prefabricated vertical drains: A case study". Geotextiles and Geomembranes, 42, Issue 4, pp302–311.
- Yildiz, A., and Uysal, F. (2015) "Numerical modelling of Haarajoki test embankment on soft clays with and without PVDs". Geomechanics and Engineering, 8, Issue 5, pp707–726.
- Zhou, Y., and Chai, J.-C. (2017) "Equivalent 'smear' effect due to non-uniform consolidation surrounding a PVD". Geotechnique, 67, Issue 5, pp410–419.

#### APPENDIX A: NOTATIONS

$a$	cyclic amplitude
$A_m$	cross-sectional area of mandrel
$b_{base}$	base width of preload in the field
$b_c$	half-width of unit cell in plane strain
$b_d$	half-width of PVD in plane strain
$b_s$	half-width of disturbed zone in plane strain
$b_t$	thickness of PVD
$b_{top}$	top width of preload in the field
$b_w$	width of PVD
$c$	cohesive intercept
$c_h$	horizontal coefficient of consolidation
$c_v$	vertical coefficient of consolidation
$C_c$	compression index

$C_k$	permeability index	$u$	excess pore water pressure
$C_s$	swelling index	$u_0$	initial excess pore water pressure
$CR$	compression ratio	$\bar{u}$	average excess pore water pressure
$CSR$	cyclic stress ratio	$\bar{U}_h$	average horizontal degree of consolidation
$d$	diameter of laboratory soil sample	$v$	velocity of flow of pore water
$D_R$	relative density	$w$	settlement
$D_{50}$	mean particle size	$w_c$	water content
$e$	void ratio	$w_L$	liquid limit
$e_0$	initial void ratio	$z$	depth below ground surface
$f$	frequency	$\gamma$	moist unit weight of soil
$F$	factor of safety	$\gamma_b$	buoyant unit weight of soil
$h$	height of laboratory soil sample	$\gamma_w$	unit weight of water
$h_e$	height of preload in the field	$\gamma^p$	plastic shear strain
$H$	thickness of soft soil layer	$\delta$	lateral displacement
$i$	hydraulic gradient	$\varepsilon_a$	axial strain
$k_{eq}$	equivalent hydraulic conductivity of PVD-improved soil	$\varepsilon_v$	volumetric strain
$k_g$	hydraulic conductivity of geotextile filter normal to the plane of the geotextile	$\sigma_c$	confining stress
$k_h$	horizontal hydraulic conductivity of natural ( <i>in situ</i> ) soil	$\sigma'_v$	vertical effective stress
$k_s$	horizontal hydraulic conductivity of soil in disturbed zone	$\sigma'_{v0}$	initial vertical effective stress
$k_{sm}$	horizontal hydraulic conductivity of soil in inner smear zone	$\sigma'_{vp}$	preconsolidation stress
$k_{tr}$	horizontal hydraulic conductivity of soil in transition zone	$\phi$	angle of shearing resistance
$k_v$	vertical hydraulic conductivity of natural ( <i>in situ</i> ) soil		
$K_0$	coefficient of lateral earth pressure at-rest		
$l_d$	length of PVD for one-way drainage and half the PVD length for two-way drainage		
$LOI$	loss on ignition		
$m$	normalised (with respect to $r_{d,eq}$ ) radius of inner smear zone		
$m_v$	coefficient of volume compressibility		
$n$	normalised (with respect to $r_{d,eq}$ ) radius of unit cell		
$OCR$	overconsolidation ratio		
$O_{95}$	apparent opening size of geotextile filter		
$PI$	plasticity index		
$PL$	plastic limit		
$p_v$	maximum value of applied total stress due to preloading		
$p'$	mean effective stress		
$q$	normalised (with respect to $r_{d,eq}$ ) radius of transition zone		
$q_c$	cone resistance		
$q_w$	discharge capacity of PVD		
$r$	radial distance measured from centre of PVD		
$r_{c,eq}$	equivalent radius of unit cell		
$r_{d,eq}$	equivalent radius of PVD		
$r_{m,eq}$	equivalent radius of mandrel		
$r_s$	equivalent radius of single disturbed zone		
$r_{sm}$	equivalent radius of inner smear zone		
$r_{tr}$	equivalent radius of transition zone		
$R_u$	excess pore water pressure ratio ( $= u/\sigma'_{v0}$ )		
$RC$	relative compaction		
$s$	centre-to-centre spacing of PVDs		
$s_u$	undrained shear strength		
$t$	time		
$T_h$	time factor for flow of pore water in horizontal direction		
$T_{max}$	maximum tension developed in reinforcement		
$T_{ult}$	ultimate tensile strength of reinforcement		